



HAL
open science

Simple approximate closed-form expressions for tracer injection in aquifer with a radially converging or diverging flow field

Dominique Thiéry

► **To cite this version:**

Dominique Thiéry. Simple approximate closed-form expressions for tracer injection in aquifer with a radially converging or diverging flow field. *Journal of Hydrology*, 2022, 608, pp.127661. 10.1016/j.jhydrol.2022.127661 . hal-03640158

HAL Id: hal-03640158

<https://brgm.hal.science/hal-03640158>

Submitted on 22 Jul 2024

HAL is a multi-disciplinary open access archive for the deposit and dissemination of scientific research documents, whether they are published or not. The documents may come from teaching and research institutions in France or abroad, or from public or private research centers.

L'archive ouverte pluridisciplinaire **HAL**, est destinée au dépôt et à la diffusion de documents scientifiques de niveau recherche, publiés ou non, émanant des établissements d'enseignement et de recherche français ou étrangers, des laboratoires publics ou privés.



Distributed under a Creative Commons Attribution - NonCommercial 4.0 International License

1 *Manuscript: HYDROL43236*

2 Simple approximate closed-form expressions for tracer injection in aquifer with a radially
3 converging or diverging flow field.

4

5 Dominique Thiéry *

6 BRGM, Division DEPA/GDR, 3 avenue Claude Guillemin, BP 36009, F-45060 Orléans cedex
7 2, France

8 * Corresponding author. Tel.: +33 6 52 27 92 64

9 E-mail addresses: dominique.thiery5@wanadoo.fr

10

11 **Abstract**

12 The exact solution for the concentration breakthrough curves resulting from a solute injection
13 in radially converging flow in an aquifer obtained using Laplace transforms has a complex
14 form difficult to compute, and cannot be given in closed-form expression. This makes it
15 difficult to use for tracer tests analysis in radial flow. To overcome this difficulty new simple
16 approximate but accurate closed-form expressions are derived in the present paper for slug
17 and continuous injections. The improvement of accuracy of these new closed-form
18 expressions is demonstrated. The paper establishes also that the breakthrough curves
19 resulting from slug injections into a radially diverging or radially converging flow are exactly
20 identical at the sampling well in domains having the same spatial extension. Solutions were
21 also derived for tracers or solutes subject to degradation.

22 The new closed-form expressions were used for the analysis of 12 field tracer tests to
23 highlight the difference in transport parameters determination compared previous
24 approximate expressions.

25

26 **Keywords:**

27 Radial flow tracer tests, Closed-form approximation, Dimensional expression, Field
28 test applications

29

30 **1 Introduction**

31 Tracer tests are widely used to determine non-reactive parameters governing transport in
32 porous media, such as the effective porosity, the retardation factor and the dispersivities.

33 Tracer tests may be performed from an injection well to a pumping well. If the flow rates in
34 the wells are small, the flow is nearly 1D Cartesian and represents the background flow

35 under natural conditions in the aquifer. There are then simple exact expressions to describe
36 the time evolution of the concentration at the pumping well corresponding to an

37 instantaneous injection of tracer (slug injection) or to a constant rate mass flux injection

38 (continuous injection). Analyzing the monitored breakthrough curve (BTC) with a software

39 such as CXTFIT (Toride et al., 1999), TRACI95 (Käss, 1998), QTRACER2 (Field, 2002),

40 TRAC (Gutierrez et al., 2013) using these 1D expressions enables to determine the transport

41 parameters. Tracer tests under natural conditions are however difficult to manage, because

42 of difficulty in determining the exact direction of flow, and the long duration of the tests

43 resulting from the generally low velocities. Tracer tests in radially converging flow are widely

44 used to overcome these difficulties, and tests in radially diverging flows can also be used for

45 some applications (Fig. 1).

46 << *Figure 1 (Schematic diagram of radially ...)* >>.

47 In both cases there are two wells: the first well located at the center of the radial flow, and the
48 second well located laterally at the radial distance r_L from the center, called the outer well. In

49 a diverging flow: the central well is an injection well where the tracer is introduced, and the

50 sampling well is located at the distance r_L . In a converging flow, it is the opposite: the tracer

51 is introduced in the outer well, and the central well is a pumping well where the tracer is

52 sampled. The domain extension may be of two types: a semi-infinite domain extending from

53 the central well to infinity, referred in this paper as an “unbounded domain”, or a bounded

54 domain extending only from the central well to the outer well. An unbounded domain would
55 seem a priori to be closer to the field reality, but as will be discussed later, the solution of the
56 convection-dispersion equation in converging flow generates a non-physical upstream
57 dispersion that is reduced when considering a bounded domain.

58 Interpretation of tracer tests in radial flow is difficult because there are no exact closed-form
59 solutions available for diverging flows, and the solutions available for converging flow, using
60 Laplace transform or Airy functions are difficult to include in an interpretation software.

61 The purpose of this paper is to establish easy to use approximate closed-form expressions
62 describing the evolution of the concentration of a tracer or solute in a radially converging or
63 diverging flow field in bounded or unbounded domain. Closed-form expressions will be also
64 established for solutes subject to degradation.

65 **2 Previous work**

66 Numerous papers addressed with different approaches the solution of radial flow tracer tests
67 in diverging or converging flow, in bounded or unbounded domain.

68 **Solutions for diverging flow only:**

69 Ogata (1958) presented the exact solution for a continuous injection in diverging flow but its
70 expression requires the integration of a rational fraction of Bessel functions of the first and
71 second kind, hence the numerical calculation of this function is very complex.

72 **Solutions for converging and diverging flow:**

73 Sauty (1980) used a numerical finite differences model to compute the BTCs, and presented
74 approximations by analytical functions and type curves for the concentration normalized by
75 the maximum concentration C/C_{\max} . However the results, which do not compare well to exact
76 solutions, are only for Péclet numbers greater than 5 or 10, depending on the selected
77 function, and for a slug injection refer only to the C/C_{\max} ratio. Welty and Gelhar (1994) gave
78 an approximate solution for high Péclet numbers. Wang and Crampon (1995) used a
79 numerical model, with an outer boundary located far from the outer well, to fit analytical
80 functions after applying correction factors to them. Their results which use a great number of

81 correcting factors are approximate, as will be seen, apply only to Péclet numbers greater
82 than 3, and also refer only to the C/C_{\max} ratio.

83 **Solutions for converging flow only:**

84 Moench (1989), using Laplace transform, presented the exact closed-form analytical solution
85 for converging flow in a bounded domain, i.e. without dispersion upstream of the injection
86 well, as pointed out by Zlotnik and Logan (1996). Moench (1995) gave solutions for
87 converging flow with double porosity. Chen et al. (1996) presented the exact solution for
88 converging flow in an unbounded domain. Their analytical solution, involving Airy functions of
89 complex arguments and Laplace inversion, are however quite difficult to compute due to the
90 numerical back-transformation of the solutions in the Laplace domain to the time domain.
91 Becker and Charbeneau (2000) presented also a solution for converging flow using Airy
92 functions and Laplace transform. Chen et al. (2002) presented a new exact solution in
93 bounded domain somewhat simpler, with Laplace transform but without Airy functions. Chen
94 et al. (2003a) analyzed the effect of the well bore mixing volume. Chen et al. (2003b) derived
95 semi-analytical solutions with a scale-dependent dispersivity.

96 **Special configurations:**

97 Wang and Zhan (2013) developed semi-analytical solutions of radial reactive solute transport
98 in an aquifer–aquitard system in diverging flow, via Laplace transform and finite Fourier
99 transform techniques and numerical inversion. Csanady (1973), Pérez Guerrero and Skaggs,
100 (2010), Natarajan, (2016) proposed various schemes where the longitudinal dispersivity is
101 not constant but increases with transport distance. Irvine et al. (2020) described a method to
102 reduce unwanted upstream dispersion in 2D discretized numerical models. Akanji and
103 Falade (2018) derived a solution to the radial transport of tracer under the influence of linear
104 drift. Their solution, which uses Tricomi-Kummer functions and requires a numerical Laplace
105 inversion, shows that the effect of the drift becomes progressively more pronounced at later
106 times. Van Genuchten (1981, 1985) presented solutions, in Cartesian coordinates, for
107 solutes involved in sequential first-order decay reactions.

108 **3 Mathematical formulation**

109 << *Nomenclature: approximatively here* >>

110 A homogeneous and isotropic aquifer, of infinite horizontal extent and constant thickness h
111 and effective porosity ω is considered. A well of negligible radius, located in this aquifer with
112 a constant injection or pumping rate, creates a steady-state diverging or converging radial
113 flow field. Tracer transport in the aquifer occurs by radial advection and by mechanical
114 dispersion. The effects of molecular diffusion and also the effects of both extraction and
115 injection well mixing volumes are considered as negligible. Tracer degradation is not
116 considered in this section, however closed-form expressions including degradation will be
117 presented in Section 7.5.

118 Two mass injection regimes are studied: a slug (or Dirac) injection where a mass M of tracer
119 is injected instantaneously, or a continuous injection where a constant mass flux q_m is
120 injected. The continuous injection corresponds to the integration over time of slug injections.

121 **3.1 Diverging flow**

122 The well injects a constant positive flow rate Q . At the initial time a mass M of tracer, or a
123 constant mass flux q_m of tracer, is injected instantaneously into the well. The concentration is
124 monitored in a sampling well situated at a distance r_L . The system is perfectly axisymmetric
125 and the mass transport equation (Sauty, 1980) is

$$126 \quad R \frac{\partial C}{\partial t} = D_L \frac{\partial^2 C}{\partial r^2} - u \frac{\partial C}{\partial r} \quad (1)$$

127 Where r is the radial distance from the well, t is the time from the start of the tracer injection,
128 C is the tracer concentration, u is the pore velocity, D_L is the longitudinal dispersion
129 coefficient, and R is the tracer retardation factor resulting from a partition coefficient k_d
130 between the liquid phase and a solid phase. The geometry being axisymmetric the
131 transverse dispersion coefficient has no influence and doesn't appear in the equation.
132 Assuming that $D_L = \alpha_L |u|$, neglecting the molecular diffusion, and expressing the velocity as
133 $u = Q / 2\pi r h \omega = A / r$, where $A = Q / 2\pi h \omega$, into eq. (1) results in:

134
$$R \frac{\partial C}{\partial t} = \alpha_L \frac{A}{r} \frac{\partial^2 C}{\partial r^2} - \frac{A}{r} \frac{\partial C}{\partial r} \quad (2)$$

135 **3.2 Converging flow**

136 The well is pumped at a constant positive flow rate Q . At the initial time a mass M of tracer,
 137 or a constant mass flux q_m of tracer, is injected in a nearby borehole at a distance r_L , without
 138 disturbing the flow field in the aquifer. The concentration is monitored in the pumped well.

139 The system is not axisymmetric and the mass transport equation (Sauty, 1980) is

140
$$R \frac{\partial C}{\partial t} = \alpha_L |u| \frac{\partial^2 C}{\partial r^2} + \frac{\alpha_T |u|}{r^2} \frac{\partial^2 C}{\partial \theta^2} - u \frac{\partial C}{\partial r} \quad (3)$$

141 where α_T is the transverse dispersivity, θ the angular coordinate, and $u = -A / r$ is negative.

142 Because the concentration in the pumped well is the average over the negligible well radius,
 143 Sauty (1977a, 1980) shows that it is possible to consider the average concentration at a
 144 radius r .

145
$$C(r, t) = \frac{1}{2\pi} \int_0^{2\pi} C(r, \theta, t) \cdot d\theta \quad (4)$$

146 Applying this transformation to eq. (3), the second term depending on θ and α_T disappears.

147 The average concentration does not depend any more on the transverse dispersivity and
 148 eq. (5), similar to eq. (2) for diverging flow, is obtained, with only a change of sign in the last
 149 term.

150
$$R \frac{\partial C}{\partial t} = \alpha_L \frac{A}{r} \frac{\partial^2 C}{\partial r^2} + \frac{A}{r} \frac{\partial C}{\partial r} \quad (5)$$

151 **3.3 Equation for both diverging and converging flow**

152 The equations for diverging and converging flow may be combined as:

153
$$R \frac{\partial C}{\partial t} = \alpha_L \frac{A}{r} \frac{\partial^2 C}{\partial r^2} - \varepsilon \frac{A}{r} \frac{\partial C}{\partial r} \quad (6)$$

154 where $\varepsilon = +1$ for diverging flow and $\varepsilon = -1$ for converging flow.

155 To obtain a dimensionless equation let the following variables:

156 $t_a = \pi r_L^2 h \omega / Q = r_L^2 / 2A =$ advection time from the injection point to the observation point

157 located at distance r_L .

158 $C_{ref} = M/(\pi r_L^2 h \omega)$ = Injected mass divided by the water volume within the distance r_L for a
159 slug injection.

160 $C_0 = q_m/Q$ = Equivalent injected concentration for a continuous mass flux injection.

161 $P = r_L / \alpha_L$ = Péclet number.

162 Using the dimensionless variables: $r_D = r / r_L$; $t_D = t / t_a$; $C_D = C/C_{ref}$, or $C_D = C/C_0$, the
163 mass transport equation eq. (6), for diverging or converging flow becomes

$$164 \quad 2R \frac{\partial C_D}{\partial t_D} = \frac{1}{P \cdot r_D} \frac{\partial^2 C_D}{\partial r_D^2} - \varepsilon \frac{1}{r_D} \frac{\partial C_D}{\partial r_D} \quad (7)$$

165 where $\varepsilon = +1$ for diverging flow and $\varepsilon = -1$ for converging flow. The only parameter of this
166 eq. (7) is the Péclet number P , not mentioning the retardation factor R which can be included
167 in t_D)

168

169 **Boundary conditions**

170 The transport boundary condition at the central well ($r_D=0$) is

171 At the central well ($r_D=0$), the boundary condition at is

$$172 \quad C_D - \frac{1}{P} \frac{\partial C_D}{\partial r_D} = F \quad \text{in diverging flow} \quad (8a)$$

$$173 \quad \frac{\partial C_D}{\partial r_D} = 0 \quad \text{in converging flow} \quad (8b)$$

174 with $F = 0$ for a slug injection and $F = 1$ for a continuous injection.

175 In an unbounded domain, the outer boundary condition ($r_D=\infty$) is

$$176 \quad \frac{\partial C_D}{\partial r_D} = 0 \quad \text{or} \quad C_D = 0 \quad (8c)$$

177 In a bounded domain, the outer boundary condition ($r_D=1$) is

$$178 \quad \frac{\partial C_D}{\partial r_D} = 0 \quad \text{in diverging flow} \quad (8d)$$

$$179 \quad C_D + \frac{1}{P} \frac{\partial C_D}{\partial r_D} = F \quad \text{in converging flow} \quad (8e)$$

180

181 **4 Unbounded domain versus bounded domain**

182 The dispersion term in eq. (6) is a Fickian diffusion process which generates dispersion in all
183 directions, downstream but also upstream. In a converging flow the upstream dispersion
184 generates mass transport upstream of the injection well, which is non-physical because
185 mechanical dispersion is due to the heterogeneity of the velocity field caused by the
186 heterogeneity of the medium. However the velocity field heterogeneity cannot lead to counter
187 flow velocity. In fact, the upstream dispersion is essentially due to the assumption that
188 dispersion D_L is equal to $\alpha_L|u|$, with α_L independent of distance. Yet it has been observed
189 that the average value of α_L between two points is clearly increasing with their distance
190 (Sauty, 1980, Pérez Guerrero and Skaggs, 2010, Chen et al. 2003b, Natarajan, 2016).

191 A method to reduce or cancel the upstream dispersion is to assume, according to Csanady
192 (1973) and Chen et al. (2003b), that the longitudinal dispersivity is not constant but increases
193 with transport distance, thus with travel time, from a small or nil initial value to a large final
194 value. However, this method requires the dispersivity-distance relationship which is seldom
195 available. Irvine et al. (2020) describe a method to reduce unwanted upstream dispersion in
196 2D discretized numerical models by setting a lower dispersivity in areas upstream of the
197 injection wells.

198 Another classic, however somewhat artificial, way to reduce the upstream dispersion is to
199 limit the modeled domain to the outer injection well which corresponds to a bounded domain.
200 In fact, this cancels the dispersivity upstream of the injection well, but not all the upstream
201 dispersion that results from the symmetric dispersion term in eq. (5).

202 To deal with this issue of bounded or unbounded domain, it has been decided in this paper,
203 for the sake of completeness, to establish closed form expressions for both the unbounded
204 and the bounded domain. A comparison of the transport parameters obtained in a tracer test
205 analysis using expressions for a bounded or unbounded domain will be presented in
206 Appendix C. Although the bounded domain applies only to converging flow, the closed-form

207 expressions have also been established in diverging flow for comparison, and for possible
208 use in particular configurations.

209 **5 Method for obtaining approximate closed-form expressions**

210 To obtain closed-form expressions easy to use and to integrate into a computer code,
211 without Airy functions or Laplace inversion, which is the main goal of this paper, an approach
212 somewhat similar to that of Wang and Crampon (1995) was used. Starting from simple
213 approximate closed-form expressions for a slug injection or a continuous injection in 1D
214 Cartesian coordinate, two correction coefficients, applied to the Péclet number P and the
215 dimensionless time t_D , were introduced into the expression to obtain a simple expressions
216 that most accurately reproduce the exact solutions.

217 Since the exact solutions, that involve Airy functions or Laplace inversions, were difficult to
218 determine, another method was used to calculate them. A finite volume groundwater flow
219 and transport numerical model was used to obtain numerically exact BTCs resulting from
220 slug or continuous injections for a wide range of Péclet numbers, from 0.1 to 1000, that will
221 be used later to determine the simple approximate closed-form expressions. The accuracy of
222 the model simulations was checked by comparing them to the available exact solutions of a
223 limited number of BTCs in converging flow, as presented in figures from the literature, mainly
224 in Moench (1989), Chen et al. (1996, 2002). The numerical model was also used to generate
225 the exact solutions in diverging flow that are not available in the literature, and to take into
226 account the tracer degradation as will be shown in Section 7.5.

227 **6 Numerical solutions in converging and diverging flow**

228 The numerical calculations were performed with MARTHE code (Thiéry, 2010, 2015b,
229 Vanderborght et al., 2005, Thiéry and Picot, 2020). In the numerical code, the mass transport
230 equation is solved numerically using a total-variation-diminishing (TVD) method implemented
231 with a flux limiter (Leonard, 1988), which produces very little numerical dispersion. Due to the
232 axisymmetric geometry the calculations were performed with a 1D radial grid. Following

233 Sauty (1977a), a non-uniform spatial discretization was implemented to ensure a constant
234 numerical Courant number. As the pore velocity decreases with the distance from the central
235 well, the grid size also decreases with distance. Four sets of BTCs were generated with the
236 model: in converging flow and in diverging flow, and both of them in bounded or unbounded
237 domain.

238 **6.1 Discretization, outer boundary condition and initial conditions**

239 In the model a fine 1D radial grid is used and the steady-state radial flow field is computed
240 first. To obtain the radial flow field a source term, injection or pumping, is set in the cell
241 located at the origin of the grid, and a constant hydraulic head is prescribed, a Dirichlet
242 condition, in the model outer limit located very far from the wells. This prescribed hydraulic
243 head automatically generates the desired radial flow. Mass transport is then computed in
244 transient state starting from an initial concentration initially equal to zero in the whole domain.
245 For an unbounded domain the outer boundary for transport was located far enough away
246 from the central well to have no influence, usually at a dimensionless radial distance r_D equal
247 to 3. For Péclet numbers as low as 0.1, or for continuous injections, the transport outer
248 boundary was located farther, at a dimensionless radial distance equal to 7. The
249 concentration was prescribed at this outer boundary, but it was verified that this boundary
250 being located far enough away, the results obtained with a no-flow boundary were identical.
251 For a bounded domain the grid extension, hence the outer boundary for transport, was
252 limited to the outer well, i.e. at a dimensionless distance r_D equal to 1. At this outer boundary,
253 a constant hydraulic head is prescribed, as was done for the unbounded domain to generate
254 the desired radial flow, and a no-flow boundary condition was set for the mass transport,
255 without prescribing the concentration. However exactly the same results were obtained
256 keeping the former quasi-infinite grid and setting a nil dispersivity in all cells located at a
257 dimensionless distance larger than 1. The dimensionless radial distance r_D equal to 3, or
258 equal to 7, was discretized in 3000 cells and the dimensionless time t_D up to 5 was divided in
259 10500 time steps.

260 **6.2 Verification of the numerical scheme and discretization in**
261 **converging flow**

262 The 1D radial numerical scheme and discretization was checked by comparison with
263 available solutions in converging flow in unbounded and bounded domains.

264 A first verification was done in unbounded domain for Péclet numbers ranging from 0.1 to
265 300. Fig. 2 illustrates that, even for Péclet numbers as small as 0.1, the numerical solutions
266 are identical to Chen et al. (1996) analytical solution as depicted in their Fig. 2.

267 << *Figure 2 (Comparison of dimensional BTCs to the Chen et al....)* >>.

268 A second verification was done in bounded domain by comparison to Moench (1996) and to
269 Chen et al. (2002) analytical solution for Péclet numbers ranging from 0.1 to 200. It is shown
270 in Appendix A that the numerical solutions are also identical to the exact analytical solution
271 (Fig. A1 and A2).

272 It was also verified numerically that, as demonstrated by Sauty (1977a, 1980), the transverse
273 dispersion has no influence. A simulation was performed, with the same numerical code, in
274 2D radial coordinates in an unbounded domain, for a Péclet number equal to 5 with a
275 transverse dispersivity equal to $0.2 \times \alpha_L$. Fig. 3 confirms that the simulated average
276 concentration along the production well radius is identical to the concentration obtained with
277 a 1D simulation without transverse dispersivity which is a further verification of the numerical
278 code accuracy. The accuracy of the solutions obtained with the numerical model having been
279 carefully verified, these numerical solutions will be called "exact solutions" from here on in
280 the paper.

281 << *Figure 3 (2D numerical simulation with transverse dispersivity...)* >>.

282 **6.3 Numerical solution for a slug injection or a continuous injection in**
283 **a diverging flow in unbounded domain**

284 The exact solutions for diverging flow being not available in the literature, they are also
285 generated with the numerical model. The accuracy of the numerical modeling being verified
286 in converging flow, it is assumed that the numerical scheme and the spatial and time
287 discretization can also be used for diverging flow using a different boundary condition. For
288 this calculation the outer boundary is set at a distance sufficient to obtain there a negligible

289 concentration, less than 1/1000 of maximum concentration. Because the flow field is
290 axisymmetric, the transverse dispersivity having no influence is not included in the
291 calculation. Fig. 4 compares the BTCs resulting from a slug injection in diverging flow and in
292 converging flow in an unbounded domain for Péclet numbers ranging from 0.1 to 100. It
293 appears, though it has not been demonstrated, that the BTCs are absolutely identical. Fig. 5
294 compares the concentrations profiles at $t_D = 0.25$ & $t_D = 0.5$ for a slug injection in diverging
295 flow and in converging flow in an unbounded domain, for a Péclet number equal to 3:
296 although the profiles are essentially different, the concentrations at the sampling well are
297 identical. This result is quite different from the results obtained by Wang and Crampon
298 (1995), who used the same outer boundary condition, probably because the radial extent of
299 their grid was too small, especially for small Péclet numbers.

300 Since the continuous injection corresponds to the integration over time of slug injections, the
301 computed BTCs in converging and in diverging flow should also be identical, which was
302 verified by our simulations. The numerical solution for BTCs curves from continuous injection
303 in diverging flow, not displayed in the paper, are exactly identical to the corresponding BTCs
304 in converging flow.

305 << Figure 4 (Comparison of the numerical solution for a slug injection...) >>.

306 << Figure 5 (Numerical simulation in converging flow and diverging flow...) >>.

307 **6.4 Numerical solution for a slug injection or a continuous injection in** 308 **bounded domain**

309 The BTCs resulting from a slug injection in bounded domain in diverging and in converging
310 flow have been computed for Péclet numbers ranging from 0.1 to 200. Fig. 6 compares the
311 BTCs obtained in diverging flow and in converging flow in a bounded domain. Similar to what
312 was obtained in unbounded domain, it appears, though it has not been demonstrated, that in
313 bounded domain also the BTCs are absolutely identical in diverging flow and in converging.
314 Fig. 7 displays the concentrations profiles at $t_D = 0.25$ & $t_D = 0.4$ for a slug injection in
315 diverging flow and in converging flow in bounded domain, for a Péclet number equal to 3. It

316 illustrates that, as in unbounded domain, although the profiles are different, the
317 concentrations at the sampling well are identical.

318 << Figure 6 (Bounded domain numerical solution in converging flow and diverging ...) >>.

319 << Figure 7 (Numerical simulation in converging flow and diverging flow...) >>.

320

321 **7 Approximate closed-form expressions**

322 As explained in Section 5, the exact solutions needed to obtain the approximate closed-form
323 expressions were obtained by numerical modeling. The exact solutions for slug injections
324 and continuous injections were successively computed with the numerical model for 20
325 values of Péclet numbers ranging from 1 to 1000, or from 0.8 to 1000, for dimensionless time
326 t_D ranging from 0 to 6. The solutions were calculated only in converging flow, as it has been
327 shown that they were identical in diverging flow. For each solution, slug injection or
328 continuous injection, a simple closed-form expression approximation F of the exact solution
329 in the form of eq. (9) is selected

$$330 \quad C_D(t_D) = F(P, t_D) \quad (9)$$

331 As in Wang and Crampon (1995) approach, two correction factors were introduced: a
332 correction factor f_T on the dimensionless time and a correction factor f_P on the Péclet number
333 to obtain a simple closed-form expression that most accurately reproduces the exact
334 solutions. The following formulation for these correction factors, depending only of the Péclet
335 number, was chosen

$$336 \quad f_T = a + b \cdot P^c \quad \text{and} \quad f_P = d + e \cdot P^f \quad (10)$$

337 In the equations the dimensionless time t_D is multiplied by f_T , and the Péclet number P is
338 divided by f_P . The reason why P is divided by f_P , rather than multiplied by f_P , is that f_P was
339 introduced as a multiplying factor on the dispersivity, hence a dividing factor on the Péclet
340 number.

341 Introducing the two correction factors of eq. (10) into eq. (9) it becomes:

342 $C_D(t_D) = F(P / f_P, f_T \cdot t_D)$ (11)

343 The unique set of 6 constants $a, b, c, d, e,$ and f is determined by optimization, using the
 344 Rosenbrock (1960) algorithm, to simultaneously reproduce as accurately as possible with eq.
 345 (11) a large set of around 20 BTCs corresponding to 20 values of the Péclet number. The
 346 optimization process maximizes the average Nash criterion (Nash and Sutcliffe, 1970) of the
 347 20 BTCs obtained by eq. (11) with respect to the corresponding exact solutions.

348 Approximate expressions are established both for an unbounded domain (Section 7.1) and
 349 for a bounded domain (Section 7.2). The improvement of the new closed-form expression,
 350 compared to available approximate expressions, is demonstrated in Section 7.3. The
 351 application of the expressions for a solute subject to interactions resulting in a retardation
 352 coefficient is described in Section 7.4. The adaption of the closed-form expressions to
 353 solutes or tracers subject to degradation is presented in Section 7.5. A comparison of the
 354 transport parameters obtained in a tracer test analysis using expressions for a bounded or
 355 unbounded domain is given in Appendix C. It highlights the large variations in dispersivity
 356 values, but also in porosity, obtained according to the choice of geometry.

357 **7.1 Approximate closed-form expressions in unbounded domain**

358 Closed-form expressions were derived in unbounded domain for a continuous injection and
 359 for a slug injection.

360 **7.1.1 Approximate closed-form expression for a continuous injection in**
 361 **unbounded domain**

362 Two 1D closed-form expressions were tried to determine which one would produce the best
 363 results. The first expression eq. (12) is the solution for a constant rate mass injection in
 364 Cartesian coordinates. It was derived by Sauty (1977a) by integration of the solution reported
 365 by Bear (1972) for a slug injection into an infinite column:

366 $C(x, t) = \frac{q_m}{2Q} \left\{ \operatorname{erfc} \left[\frac{(x-ut)}{\sqrt{4D_L t}} \right] - \exp \left(\frac{x}{\alpha_L} \right) \cdot \operatorname{erfc} \left[\frac{(x+ut)}{\sqrt{4D_L t}} \right] \right\}$ (12)

367 The second expression considered, eq. (13), is a simplification of eq. (12) obtained by
 368 dropping its second term:

369 $C(x, t) = \frac{q_m}{2Q} \operatorname{erfc} \left[\frac{(x-ut)}{\sqrt{4D_L t}} \right]$ (13)

370 The results obtained with this expression turned out to be significantly closer to the exact
371 solution, especially for Péclet numbers smaller than 3

372 In radial flow, at a distance $r = r_L$, considering the “average” pore velocity u_a defined as

373 $u_a = \frac{r_L}{t_a} = \frac{Q}{\pi h \omega r_L}$; $D_L = \alpha_L \cdot u_a$. The equivalent formulation of eq. (13) in radial

374 coordinate in dimensionless form is

375 $C_D(t_D) = 0.5 \cdot \operatorname{erfc} \left[\sqrt{\frac{P}{4t_D}} (1 - t_D) \right]$ (14)

376 This formulation is only a crude approximation of the exact solution. Introducing the two
377 correction factors f_T and f_P , eq. (14) becomes:

378 $C_D = 0.5 \cdot \operatorname{erfc} \left[\sqrt{\frac{P/f_P}{4f_T \cdot t_D}} (1 - f_T \cdot t_D) \right]$ (15)

379 As explained before, the optimal set of 6 constants $a, b, c, d, e,$ and f is determined by
380 optimization to simultaneously reproduce as accurately as possible with eq. (15) the 20 BTCs
381 corresponding to 20 values of the Péclet number. With this unique set of 6 constants a very
382 good match was obtained for Péclet numbers ranging from 0.8 to 1000, and t_D ranging from 0
383 to 6 (See Fig. 8). The lowest Nash criterion of all curves is 0.9994.

384 << *Figure 8 (Continuous injection, converging flow and diverging flow...)* >>.

385 The equations obtained for the correcting factors for a continuous injection in converging or
386 diverging flow in unbounded domain are

387 $f_T = 1.00627 - 0.44829 \cdot P^{-0.73712}$ (16a)

388 $f_P = 1.44488 - 0.21574 \cdot P^{-0.78005}$ (16b)

389 **7.1.2 Approximate closed-form expression for a slug injection in unbounded** 390 **domain**

391 Bear (1972) shows that the analytical solution for a slug injection into an infinite column is

392 $C(x, t) = \frac{M}{\omega h w \sqrt{4\pi D_L t}} \cdot \exp \left[-\frac{(x-ut)^2}{4D_L t} \right]$ (17)

393 where w is the width of the horizontal column.

394 In radial flow, at a distance $x = r_L$ and using u_a , the equivalent formulation in radial coordinate
395 is

$$396 \quad C(r_L, t) = \frac{Mu_a}{Q\sqrt{4\pi\alpha_L u_a t}} \cdot \exp\left[-\frac{(r_L - u_a t)^2}{4\alpha_L u_a t}\right] \quad (18)$$

397 and in dimensionless variables

$$398 \quad C_D(t_D) = \sqrt{\frac{P}{4\pi t_D}} \cdot \exp\left[-\frac{P}{4t_D}(1 - t_D)^2\right] \quad (19)$$

399 However the derivative with respect to dimensionless time t_D of eq. (14), which gave a very
400 good match for a continuous injection, is

$$401 \quad C_D(t_D) = 0.5 \sqrt{\frac{P}{4\pi t_D}} \cdot \frac{(t_D+1)}{t_D} \cdot \exp\left[-\frac{P}{4t_D}(1 - t_D)^2\right] \quad (20)$$

402 Introducing the correction factors f_P and f_T , eq. (20) becomes:

$$403 \quad C_D(t_D) = 0.5 \cdot f_T \sqrt{\frac{P/f_P}{4\pi f_T t_D}} \cdot \frac{(f_T t_D + 1)}{f_T t_D} \cdot \exp\left[-\frac{P/f_P}{4f_T t_D}(1 - f_T t_D)^2\right] \quad (21)$$

404 The leading factor f_T introduced into the first term is necessary to have an integral from $t_D=0$
405 to ∞ equal to 1, i.e. to conserve mass.

406 As for the continuous injection, another unique set of 6 constants a , b , c , d , e , and f was
407 determined by optimization to obtain the closest approximation of the 20 exact solutions for
408 slug injections. Again a very good match is obtained for Péclet numbers ranging from 1 to
409 1000, and t_D ranging from 0 to 6 (See Fig. 9). The fit obtained with eq. (21) is significantly
410 better than that obtained when fitting eq. (19) that could have seemed more natural. The
411 lowest Nash criterion of all curves is 0.9922.

412 << Figure 9 (Slug injection in converging flow or diverging flow...) >>.

413 The equations obtained for the correcting factors for a slug injection in converging or
414 diverging flow in unbounded domain are:

$$415 \quad f_T = 1.00092 - 0.45272 \cdot P^{-0.87334} \quad (22a)$$

$$416 \quad f_P = 1.51016 - 0.3189 \cdot P^{-0.09496} \quad (22b)$$

417

418 **7.2 Approximate closed-form expressions in bounded domain**

419 In the same manner as for an unbounded domain, closed-form expressions have been
420 determined for a continuous injection and for a slug injection in bounded domain.

421 **7.2.1 Approximate closed-form expression for a continuous injection in** 422 **bounded domain**

423 Among the 1D closed-form expressions that were tried, it is the solution for a step injection at
424 fixed concentration in 1D Cartesian coordinates that produces the best results. It is Ogata
425 and Banks (1961) equation:

$$426 \quad C_D(t_D) = 0.5 \left\{ \operatorname{erfc} \left[\sqrt{\frac{P}{4t_D}} (1 - t_D) \right] + \exp(P) \cdot \operatorname{erfc} \left[\sqrt{\frac{P}{4t_D}} (1 + t_D) \right] \right\} \quad (23)$$

427 This equation differs from equation (11) by a plus sign in front of the term $\exp(\cdot) \cdot \operatorname{erfc}(\cdot)$ instead
428 of a minus sign.

429 Introducing the correction factors f_P and f_T , eq. (23) becomes

$$430 \quad C_D(t_D) = 0.5 \left\{ \operatorname{erfc} \left[\sqrt{\frac{P/f_P}{4f_T \cdot t_D}} (1 - f_T \cdot t_D) \right] + \exp(P / f_P) \cdot \operatorname{erfc} \left[\sqrt{\frac{P/f_P}{4f_T \cdot t_D}} (1 + f_T \cdot t_D) \right] \right\} \quad (24)$$

431 After determination of the optimal set of 6 constants a , b , c , d , e , and f a very good match is
432 obtained for Péclet numbers ranging from 2 to 1000 (See Fig. 10). However, the fit is not
433 quite as good for Péclet numbers lower than 2. The average Nash criterion for the 20 curves
434 is 0.9998, and the lowest criterion is 0.9988.

435 << Figure 10 (Continuous injection, converging flow and diverging flow...Bounded) >>.

436 The equations obtained for the correcting factors for a continuous injection in converging flow
437 in bounded domain are

$$438 \quad f_T = 1.17097 - 0.20663 \cdot P^{-1.87515} \quad (25a)$$

$$439 \quad f_P = 1.43094 - 0.96565 \cdot P^{-0.47269} \quad (25b)$$

440 **7.2.2 Approximate closed-form expression for a slug injection in bounded**
441 **domain**

442 Several classic closed-form expressions were tried. The derivative versus time of Ogata and
443 Banks (1961) equation for a step injection in 1D Cartesian coordinate, Lenda and Zuber
444 (1970), that was used by Sauty (1980):

445
$$C_D(t_D) = \sqrt{\frac{P}{4\pi}} \cdot t_D^{-3/2} \cdot \exp\left[-\frac{P}{4t_D}(1 - t_D)^2\right] \quad (26)$$

446 did not result in a close match for all Péclet numbers after optimization of the set of 6
447 constants. The curves for low Péclet numbers were not modeled accurately. The selected
448 closed-form expression is equation (18) for a slug injection in 1D Cartesian coordinate (Bear
449 1972). After determination of the optimal set of 6 constants a , b , c , d , e , and f , a very good
450 match is obtained for Péclet numbers ranging from 1 to 1000 (See Fig. 11). For the sake of
451 readability, the curves for Péclet numbers from 200 to 1000 do not appear in Fig. 11, but they
452 are also very accurately reproduced. The average Nash criterion for the 20 curves is 0.9993,
453 and the lowest Nash criterion is 0.9984.

454 << Figure 11 (Slug injection in converging flow or diverging flow...) >>.

455
$$C_D(t_D) = f_T \sqrt{\frac{P/f_P}{4\pi f_T \cdot t_D}} \cdot \exp\left[-\frac{P/f_P}{4f_T \cdot t_D}(1 - f_T \cdot t_D)^2\right] \quad (27)$$

456 The equations obtained for the correcting factors for a slug injection in converging flow in
457 bounded domain are:

458
$$f_T = 0.99003 + 1.29039 \cdot P^{-0.72566} \quad (28a)$$

459
$$f_P = 1.51514 - 0.89053 \cdot P^{-0.29830} \quad (28b)$$

460 **7.3 Improvement of the new closed-form expressions compared to available**
461 **expressions**

462 The improvement of the new closed-form expressions developed in the present paper has
463 been demonstrated by comparison to two approximate closed-form available in radial flow:
464 the closed-form described by Sauty (1980) for a slug injection in converging flow, and the
465 closed-form described by Wang and Crampon (1995) for the whole BTC duration. The

466 comparison is detailed in Appendix B. Fig. B1 and B2 show that the new closed-form
 467 expressions are significantly closer to the exact solutions.

468 **7.4 Expressions for a solute with a retardation factor**

469 The closed-form expressions applies also to solutes or tracers having a retardation factor R
 470 resulting from a partition coefficient k_d between the liquid phase and a solid phase. In
 471 equation (6), setting $R = 1$ and $\omega' = R \cdot \omega$, which corresponds to $A' = A / R$, leaves the
 472 equation unchanged. It is then possible to use all the derived expressions, replacing ω by
 473 $R \cdot \omega$, to obtain the concentration for a solute with a known retardation factor equal to R. On
 474 the other hand, using the original dimensionless expressions to determine the unknown
 475 transport parameters ω and α_L from a tracer test, would yield the right value for α_L , but a
 476 value of ω multiplied by R. It would then be impossible to determine the value of the
 477 retardation factor.

478 **7.5 Expressions for a solute subject to degradation**

479 The closed-form expressions may be adapted easily for solutes or tracers subject to an
 480 exponential decay during transport as $C_0 e^{-\frac{t}{T_g}}$, T_g being the first-order decay time constant
 481 for the mobile phase. Assuming the same decay time constant in the solid phase, eq. (6)
 482 becomes:

$$483 \quad R \frac{\partial C}{\partial t} = \alpha_L \frac{A}{r} \frac{\partial^2 C}{\partial r^2} - \varepsilon \frac{A}{r} \frac{\partial C}{\partial r} - R \frac{C}{T_g} \quad (29)$$

484 Using the dimensionless decay time constant: $T_{gD} = T_g / t_a$, the dimensionless equivalent of
 485 eq. (7) is

$$486 \quad 2R \frac{\partial C_D}{\partial t_D} = \frac{1}{P \cdot r_D} \frac{\partial^2 C_D}{\partial r_D^2} - \varepsilon \frac{1}{r_D} \frac{\partial C_D}{\partial r_D} - 2R \frac{C_D}{T_{gD}} \quad (30)$$

487 It can be verified that if $C_D(r_D, t_D)$ is solution of eq. (7) then

$$488 \quad C'_D(r_D, t_D) = C_D(r_D, t_D) \cdot e^{-\frac{t_D}{T_{gD}}} \text{ is solution of eq. (30)}$$

489 $C_D = C'_D \cdot e^{\frac{t_D}{T_{gD}}}$, (31a), $\frac{\partial C_D}{\partial t_D} = \frac{\partial C'_D}{\partial t_D} \cdot e^{\frac{t_D}{T_{gD}}} + \frac{C'_D}{T_{gD}} \cdot e^{\frac{t_D}{T_{gD}}}$ (31b),

490 $\frac{\partial C_D}{\partial r_D} = \frac{\partial C'_D}{\partial r_D} \cdot e^{\frac{t_D}{T_{gD}}}$ (31c), $\frac{\partial^2 C_D}{\partial r_D^2} = \frac{\partial^2 C'_D}{\partial r_D^2} \cdot e^{\frac{t_D}{T_{gD}}}$ (31d)

491 Introducing eqs. (31a-31d) into eq. (7) and dividing by $e^{\frac{t_D}{T_{gD}}}$ results in eq. (30). This proves

492 that using the new closed-form expressions derived in this paper that are very close to

493 solution of eq. (7), and multiplying them by $e^{-\frac{t_D}{T_{gD}}}$ gives approximate closed-form

494 expressions integrating degradation, provided that the boundary conditions are also

495 multiplied by $e^{-\frac{t_D}{T_{gD}}}$. This applies to the slug injections, however for continuous injections it

496 would apply only if the solute is degraded with the same decay rate before being injected,

497 which is usually not verified, as bacterial degradation occurs only in the aquifer.

498 Fig. 12 refers to the BTCs resulting from a slug injection in converging or diverging flow in an

499 unbounded domain for two Péclet numbers and various decay time constants. It shows that

500 the closed-form expression applies accurately to solutes subject to exponential decay.

501 << *Figure 12 (Slug injection with degradation ...)* >>.

502 It has also been verified that for a bounded domain the equivalent expression applies also

503 with the same accuracy.

504 **8 Application to field tracer tests**

505 The new closed-form expression established in this paper for a slug injection, has been

506 applied for the interpretation of a set of tracer tests, i.e. for determining their dispersivity and

507 kinematic porosity by calibration. It was thus possible to quantify the improvement obtained

508 by using this expression rather than other approximate expressions. The set consists of

509 twelve tracer tests, mostly performed in alluvial formations. Tracer tests #1 through #8 come

510 from Gutierrez et al. (2012). The BTCs data relative to these tracer tests are provided as

511 “Supplementary material”. The main characteristics of the tests (distance to well, formation

512 thickness, pumping rate, test duration) are gathered in Table 1. The distance from the
 513 injection point to the pumping well is most of the time quite small (median value is 14 meters)
 514 with only one exception. The formations thickness are also small (median thickness is 9.3 m)
 515 and the total duration of the tests usually ranges from 1 day to 2 days, with the exception of
 516 two much longer tests. Unfortunately the injected masses were not known.

517 <<< Table 1 >>>

518 Using the Rosenbrock optimization method for determining the optimal kinematic porosity
 519 and dispersivity, the BTCs of these twelve tracer tests were reproduced successfully with the
 520 new closed-form formulation in unbounded domain, eq. (21, 22a, 22b). The median Nash
 521 and Sutcliffe criterion is 0.977 with only one value below 0.9. The calibrated kinetic porosity,
 522 dispersivity and injected mass values are given in Table 2. The Péclet numbers obtained are
 523 rather small (median value is 4.3) and only one value is above 10.

524 <<< Table 2 >>>

525 Two approximate expressions for a slug injection in converging flow were used for
 526 comparison: the expressions described by Sauty (1980) and by Wang and Crampon (1995).
 527 Sauty's (1980) expression is eq. (26), the derivative versus time of Ogata and Banks (1961)
 528 equation for a step injection in 1D Cartesian coordinate (Lenda and Zuber, 1970), without
 529 correction factors. The Wang and Crampon (1995) equation for a radially convergent slug
 530 injection, for the whole BTC, is based on eq. (19), i.e. the solution of a slug injection in 1D
 531 Cartesian coordinate with corrections factors. It is valid only for Péclet numbers greater than
 532 3:

$$533 \quad C_D(t_D) = K \sqrt{\frac{P/f_P}{4\pi t_D/f_T}} \cdot \exp \left[-\frac{P/f_P}{4t_D/f_T} (1 - t_D/f_T)^2 \right]$$

534 with

535 $K =$ Normalization constant

$$536 \quad f_T = 2 \cdot (0.503 - 0.33/P) \quad \text{if } P \leq 100 \quad \text{else} \quad f_T = 1$$

$$537 \quad f_p = 1.32 - 1.116/P$$

538 The twelve BTCs were also reproduced successfully using both these approximate
539 expressions, with comparable Nash coefficients. However the calibrated values of the kinetic
540 porosity and of the dispersivity, given in Table 3 for the Wang and Crampon (1995) equation,
541 differ significantly from those obtained using the new closed-form expression of this paper,
542 which is extremely close to the exact solution. Using the formulation of Wang and Crampon
543 (1995), both of these parameters are overestimated. The median value of the overestimation
544 is 19.9% for dispersivity and only 4.4% for kinematic porosity. Fig. 13 shows that, as
545 expected, it is for small Péclet numbers that the new closed-form expression provides more
546 accuracy, where the overestimation of the dispersivity was the largest.

547 <<< Table 3 >>>

548 << Figure 13 (Twelve tracer tests: kinematic porosity...) >>.

549 Sauty's (1980) approximation heavily overestimates the dispersivity and kinematic porosity.
550 The median value of these two parameters overestimation is 69% and 67% respectively.
551 However Sauty's (1980) approximate formulation was selected after comparison to a
552 numerical modeling using an outer boundary condition not clearly documented, but
553 apparently corresponding to a bounded domain. Therefore another comparison was made
554 with the kinematic porosity and dispersivity obtained with the new closed-form expression of
555 this paper in a bounded domain, eq. (27, 28a, 28b). The deviations are then smaller: the
556 median value of the overestimation is reduced to 15.4% for dispersivity, and to 23.2% for
557 kinematic porosity.

558 **9 Summary and conclusions**

559 This paper derived simple accurate approximate closed-form expressions for tracer injection
560 in aquifer with a radially converging or diverging flow in a bounded or unbounded domain.
561 Starting from approximate closed-form expressions for a slug injection or a continuous
562 injection in 1D Cartesian coordinate, two correction coefficients, depending only on the
563 Péclet number, were introduced into this expression to obtain new closed-form expressions
564 that most accurately reproduce the exact solutions. The conditions of application of these

565 expressions are that the aquifer must have homogeneous properties and a uniform
 566 thickness, and the central pumping (or injection) well must have a negligible radius.
 567 Longitudinal dispersion is taken into account, but the molecular diffusion is neglected.
 568 Transverse dispersion does not appear in the expressions because it has no influence. The
 569 closed-form expressions may be used for a tracer having a retardation factor and subject to
 570 exponential degradation.

571 An interesting result, obtained by the numerical simulations, is that for a given set of
 572 parameters, a BTC at the sampling well is identical in diverging or in converging flow. This
 573 applies in unbounded domain and also in bounded domain.

574 Using the 4 following dimensionless numbers:

575 $t_D = t \cdot Q / (\pi r_L^2 h \omega)$ Dimensionless time,

576 $P = r_L / \alpha_L$ Péclet number,

577 $C_D = C \cdot Q / q_m$ Dimensionless concentration for a continuous injection, or

578 $C_D = C \cdot \pi r_L^2 h \omega / M$ Dimensionless concentration for a slug injection,

579 the approximate closed-form, for Péclet number ranging from 1 to 1000, and dimensionless
 580 time ranging from 0 to 5, are:

581 **Unbounded domain**

582 Slug injection:

583
$$C_D(t_D) = 0.5 \cdot f_T \sqrt{\frac{P/f_P}{4\pi f_T t_D}} \cdot \frac{(f_T \cdot t_D + 1)}{f_T \cdot t_D} \cdot \exp \left[-\frac{P/f_P}{4f_T \cdot t_D} (1 - f_T \cdot t_D)^2 \right] \cdot e^{-\frac{t_D}{T_{gD}}}$$

584 $f_T = 1.00092 - 0.45272 \cdot P^{-0.87334}$

585 $f_P = 1.51016 - 0.3189 \cdot P^{-0.09496}$

586 (When there is no degradation, $T_{gD} = \infty$ and the last term is dropped.)

587 Continuous injection:

588
$$C_D = 0.5 \cdot \operatorname{erfc} \left[\sqrt{\frac{P/f_P}{4f_T t_D}} (1 - f_T \cdot t_D) \right]$$

589 $f_T = 1.00627 - 0.44829 \cdot P^{-0.73712}$

590 $f_p = 1.44488 - 0.21574 \cdot P^{-0.78005}$

591 **Bounded domain**

592 These expressions in a bounded domain can be used for tracer tests in converging flow, they
 593 would not be appropriate in diverging flow.

594 Slug injection:

595
$$C_D(t_D) = f_T \sqrt{\frac{P/f_P}{4\pi f_T t_D}} \cdot \exp\left[-\frac{P/f_P}{4f_T t_D} (1 - f_T \cdot t_D)^2\right] \cdot e^{-\frac{t_D}{T_{gD}}}$$

596 $f_T = 0.99003 + 1.29039 \cdot P^{-0.72566}$

597 $f_p = 1.51514 - 0.89053 \cdot P^{-0.29830}$

598 Continuous injection:

599
$$C_D(t_D) = 0.5 \left\{ \operatorname{erfc} \left[\sqrt{\frac{P/f_P}{4f_T t_D}} (1 - f_T \cdot t_D) \right] + \exp(P/f_P) \cdot \operatorname{erfc} \left[\sqrt{\frac{P/f_P}{4f_T t_D}} (1 + f_T \cdot t_D) \right] \right\}$$

600 $f_T = 1.17097 - 0.20663 \cdot P^{-1.87515}$

601 $f_p = 1.43094 - 0.96565 \cdot P^{-0.47269}$

602 The new closed-form formulation for a slug injection in unbounded domain has been applied

603 to twelve radially convergent tracer tests. The mass transfer parameters obtained were

604 compared to those obtained by two approximate methods: Sauty's (1980) formulation and

605 the formulation of Wang and Crampon (1995). It appeared that Sauty's (1980) approximate

606 formulation results in overestimations of both the kinematic porosity and the dispersivity.

607 Using the approximate formulation of Wang and Crampon (1995) also overestimates

608 dispersivity, but to a lesser extent.

609 It has been shown that by choosing a bounded domain, to reduce the spurious upstream

610 dispersion, instead of an unbounded domain corresponding to the real geometry, significantly

611 different values are obtained for the dispersivity, but also for the porosity. These differences

612 however decrease for large Péclet numbers. It has also been shown that both schemes can

613 reproduce the BTC equally well; therefore, the analysis of the BTC alone does not allow the

614 selection of the most appropriate scheme.

615

616 **Acknowledgements**

617 The author are grateful to T. Klinka from BRGM for providing field tracer tests data to apply
618 the developed solutions, and to Dr. H.M. Kluijver for revising the final version of the English
619 text.

620 **Funding information**

621 This research was conducted by the French Geological Survey (BRGM), and was funded by
622 internal research projects.

623

624 **Appendix**

625 **Appendix A. Validation of our 1D radial numerical scheme, discretization and outer** 626 **boundary conditions in bounded domain**

627 Our 1D radial numerical scheme and discretization was validated in bounded domain in
628 converging flow by comparison to Chen et al. (2002) analytical solution as depicted in their
629 Fig. 2 and Fig. 4. Fig. A1 and Fig A2 show that the numerical calculations, with the selected
630 spatial and temporal discretization and outer boundary condition reproduce accurately the
631 exact analytical solution of Chen et al. (2002) for Péclet numbers ranging from 0.1 to 200.

632 << *Figure A1 (Comparison of dimensional BTCs...Péclet from 0.1 to 25)* >>.

633 << *Figure A2 (Comparison of dimensional BTCs...Péclet from 25 to 200)* >>.

634

635 **Appendix B. Evaluating the improvement of the new closed-form expressions**

636 The improvement of the new closed-form expressions developed in this paper is
637 demonstrated by comparison to the two approximate closed-form available for the BTC
638 resulting from a slug injection in radial flow: Sauty's (1980) closed-form for a slug injection in
639 converging flow, and the closed-form described by Wang and Crampon (1995) for the whole
640 BTC duration. The equations corresponding to these approximate expressions are given in
641 Section 8.

642 Sauty's (1980) approximation for a slug injection in converging flow

643 In the numerical model used by Sauty (1980) to select its approximate expression, the outer
644 boundary condition although not clearly documented corresponds apparently to a bounded
645 domain. For this reason their approximation was compared to the solution in a bounded
646 domain and the closeness to their solution was compared the new closed-form in a bounded
647 domain.

648 Fig. B1 shows that the new closed-form expression in bounded domain, eq. (27, 28a, 28b), is
649 significantly closer to the exact solution than Sauty's (1980) expression. This is true as well
650 for small Péclet numbers not exceeding 3 as for large values exceeding 30.

651 << *Figure B1 (Comparison to Sauty's (1980) approximate solution)* >>.

652 Wang and Crampon (1995) approximation

653 Wang and Crampon (1995) used a numerical model in unbounded domain to fit their
654 expressions. Among the four expressions, ascending part of BTC or whole BTC, converging
655 or diverging, only the two expressions for the whole BTC were selected and compared to the
656 single exact solution. The closeness of their expressions, valid for Péclet number greater
657 than or equal to 3, were compared to the single new closed-form in unbounded domain.

658 In unbounded domain also, Fig. B2 shows that the new closed-form expression, eq. (21, 22a,
659 22b), is much closer to the exact solution than Wang and Crampon (1995) expression. The
660 difference is considerable for small Péclet numbers not exceeding 3, which are below the
661 limit of validity of their expression, but is also significant for larger values. The difference
662 decreases, however, for large values exceeding 30.

663 << *Figure B2 (Comparison to Wang and Crampon (1995) approximate solution)* >>.

664

665 **Appendix C. Comparison of the transport parameters obtained in a tracer test analysis**
666 **using expressions for a bounded or unbounded domain**

667 The transport parameters, kinematic porosity and dispersivity, obtained from the analysis of a
668 tracer test, depend on the assumption chosen for the domain: bounded or unbounded.

669 To analyze the sensitivity to this assumption, the dimensionless BTCs for slug injections
670 were calculated with the exact bounded domain solution for 20 values of Péclet numbers,
671 corresponding to given values of kinematic porosity and dispersivity.
672 These 20 BTCs are assumed to represent actual tracer tests. Using the exact solution
673 corresponding to the alternative assumption of an unbounded domain, the 20 BTCs are
674 analyzed to determine the corresponding kinematic porosity and dispersivity. It can be seen
675 from Fig. C1 that all BTCs corresponding to Péclet numbers greater than or equal to 1.5
676 could be reproduced very accurately with the unbounded domain solution, but with transport
677 parameters different from the original parameters. This shows that the sole analysis of a BTC
678 cannot help to determine which geometry, bounded or not, should be selected. Fig. C2
679 shows the changes in the initial parameters required to reproduce the BTCs. It appears that
680 in the unbounded domain, the corresponding calibrated dispersivity is decreased by 50%,
681 20%, and 8% respectively for Péclet numbers equal to 1.5, 10 and 30. The corresponding
682 calibrated kinematic porosity is decreased by 38%, 15% and 7% for these same Péclet
683 numbers. The reason for the decrease in dispersivity is that without upstream dispersion, the
684 BTCs are less dispersed, especially for small Péclet numbers. The decrease in kinematic
685 porosity is also explained by the fact that without upstream dispersion, the bulk advection
686 velocity is increased, resulting in a decrease in porosity.

687 << *Figure C1 (Exact solution in bounded domain: calibration in unbounded domain)* >>.

688 << *Figure C2 (Exact solution in bounded domain: modification of the porosity ...)* >>.

689

690 **References**

- 691 Akanji, L.T., and Falade, G.K., 2018 - Closed-Form Solution of Radial Transport of Tracers in
692 Porous Media Influenced by Linear Drift. *Energies* 2019, 12(1), 29;
693 <https://doi.org/10.3390/en12010029>
694 Bear, J., *Dynamics of Fluids in Porous Media*, Elsevier, New York, 1972.

695 Becker, M.W., Charbeneau, R.J., 2000. Erratum: first-passage-time transfer functions for
696 groundwater tracer tests conducted in radially convergent flow. *J. Contam. Hydrol.* 45,
697 361–372.

698 Chen, J.S., Liu, C.W., Chen, C.S., Yeh, H.D., 1996. A Laplace transform solution for tracer
699 test in a radially convergent flow with upstream dispersion. *J. Hydrol.* 183, 263–275.

700 Chen, J. S., C. W. Liu, and C. M. Liao, 2002. A novel analytical power series solution for
701 solute transport in a radially convergent flow field, *J. Hydrol.*, 266, 120–138.

702 Chen J.-S., Liu C.-W., Chen C.-S., Liao C.-M., 2003a. Effect of well bore mixing volume on
703 non-axisymmetrical transport in a convergent radial tracer test. *J. Hydrol.* 277(1), 61-73.
704 [https://doi.org/10.1016/S0022-1694\(03\)00082-9](https://doi.org/10.1016/S0022-1694(03)00082-9)

705 Chen, J.-S., Liu, C.-W., Hsu, H.-T., and Liao, C.-M., 2003b. A Laplace transform power
706 series solution for solute transport in a convergent flow field with scale-dependent
707 dispersion, *Water Resour. Res.*, 39(8), 1229, doi:10.1029/2003WR002299.

708 Csanady, G.T., 1973. *Turbulent Diffusion in the Environment*. D. Reidel Publishing Company,
709 Dordrecht, Holland. DOI:10.1007/978-94-010-2527-0

710 Field, M., 2002. The QTRACER2 program for tracer-breakthrough curve analysis for tracer
711 tests in karstic aquifers and other hydrologic systems; EPA/600/R-02/001.

712 Gutierrez, A., Klinka, T., Thiéry, D., Buscarlet, E., Binet, S., et al. 2013. TRAC, a
713 collaborative computer tool for tracer-test interpretation. 6th International Conference on
714 Tracers and Tracing Methods, Jun 2011, Oslo, Norway. 8 p., EPJ Web of Conferences
715 50, 03002 (2013)
716 doi.org/10.1051/epjconf/20135003002

717 Gutierrez, A., Klinka, T., Thiéry, D., 2012 - Manuel d'utilisation de TRAC : Aide à
718 l'interprétation de traçages en milieux poreux. BRGM report RP-60660-FR (*in French*).
719 <http://infoterre.brgm.fr/rapports/RP-60660-FR.pdf>

720 Irvine, D.J., Werner, A.D., Ye, Y., A. Jazayeri, A., 2020 - Upstream Dispersion in Solute
721 Transport Models: A Simple Evaluation and Reduction Methodology. *Groundwater journal*
722 59(2). doi.org/10.1111/gwat.13036

723 Käss, W., 1998. Tracing Technique in Geohydrology; A. A. Balkema, Rotterdam, Brookfield,
724 Vt., 581 p.

725 Lenda, A. & Zuber, A., 1970 - Tracer dispersion in groundwater experiments. In: *Isotope*
726 *Hydrology*, (619-641). International Atomic Energy Agency, Vienna.

727 Leonard, B.P., 1988. Universal Limiter for transient interpolation modeling of the advective
728 transport equations: the ULTIMATE conservative difference scheme, NASA Technical
729 Memorandum 100916 ICOMP-88-11.

730 Moench, A.F., 1989. Convergent radial dispersion: a Laplace transform solution for aquifer
731 tracer testing. *Water Resour. Res.* 25 (3), 439–447.

732 Moench, A.F., 1995. Convergent radial dispersion in a double-porosity aquifer with fracture
733 skin: analytical solution and application to a field experiment in fractured chalk. *Water*
734 *Resour. Res.* 31 (8), 1823–1835.

735 Nash, J. E. and Sutcliffe, J. V., 1970. River flow forecasting through conceptual models part I
736 — A discussion of principles, *J. Hydrol.*, 10(3), 282–290, [https://doi.org/10.1016/0022-](https://doi.org/10.1016/0022-1694(70)90255-6)
737 [1694\(70\)90255-6](https://doi.org/10.1016/0022-1694(70)90255-6)

738 Natarajan, N., 2016. Effect of distance-dependent and time-dependent dispersion on non-
739 linearly sorbed multispecies contaminants in porous media, *ISH Journal of Hydraulic*
740 *Engineering*, 22:1, 16-29, DOI: 10.1080/09715010.2015.1043597

741 Ogata, A., Dispersion in porous media, Ph.D. thesis, Northwestern Univ., Evanston, Ill.,
742 1958.

743 Ogata, A. et Banks, R.B., 1961. A solution of the differential equation of longitudinal
744 dispersion in porous media. *U.S. Geol. Surv., Prof. Pap.* 411-A.

745 Pérez Guerrero, J.S., Skaggs, T.H., 2010. Analytical solution for one-dimensional advection-
746 dispersion transport equation with distance-dependent coefficients. *J. Hydrol.* 390(1-2),
747 57-65. <https://doi.org/10.1016/j.jhydrol.2010.06.030>

748 Rosenbrock, H.H., 1960. An automatic method for finding the greatest or the least value of a
749 function; *Computer journal* 3.3., p. 175-184, Oct. 1960.

750 Sauty, J.-P., 1977a. Contribution à l'identification des paramètres de dispersion dans les
751 aquifères par l'interprétation des expériences de traçage, D.Ing. Thesis, Univ. Sci. et Méd.
752 de Grenoble, France (*in French*).

753 Sauty, J.-P. 1978 - Identification des paramètres du transport hydrodispersif dans les
754 aquifères par interprétation de traçages en écoulement cylindrique convergent ou
755 divergent. J. Hydrol., 39 (1-2) 69--103. [https://doi.org/10.1016/0022-1694\(78\)90115-4](https://doi.org/10.1016/0022-1694(78)90115-4)

756 Sauty, J.-P., 1980. An analysis of hydrodispersive transfer in aquifers. Water Resour. Res.
757 16 (1), 145–158.

758 Thiéry, D., 2010. Groundwater Flow Modeling in Porous Media Using MARTHE. *in "Modeling*
759 *Software Volume 5, Chapter 4, pp. 45-60 • Environmental Hydraulics Series". Tanguy J.M.*
760 (Ed.) – Wiley Editions/ISTE London. ISBN: 978-1-84821-157-5.

761 Thiéry, D., 2015b. Modélisation 3D du transport de masse et du transfert thermique avec le
762 code de calcul MARTHE – version 7.5. Rapport BRGM/RP-64765-FR, 324 p., 158 fig. (*in*
763 *French*). <http://infoterre.brgm.fr/rapports/RP-64765-FR.pdf>

764 Thiéry, D. and Picot-Colbeaux, G., 2020 – Guidelines for MARTHE v7.8 computer code for
765 hydro-systems modelling (English version). Report BRGM/RP-69660-FR, 246 p., 177 fig.
766 <http://infoterre.brgm.fr/rapports//RP-69660-FR.pdf>

767 Toride, N., Leij, F.J., Van Genuchten, M.Th., 1999. The CXTFIT code for estimating transport
768 parameters from laboratory or field tracer experiments. Version 2.1, Research Report
769 n°137, U.S. Salinity Lab., Riverside, CA.

770 Vanderborght J., Kasteel J., Herbst M., Javaux M., Thiéry D., Vanclooster M., Mouvet C.,
771 Vereecken H., 2005 - A set of Numerical Models for Simulating Flow and Transport in
772 Soils Using Analytical Solutions. Vadose Zone J 2005 4(1): p. 206-221.
773 <https://doi.org/10.2136/vzj2005.0206>

774 Van Genuchten, M.Th, 1985. Convective-dispersive transport of solutes involved in
775 sequential first-order decay reactions. Computers & Geosciences, 11(2): 129-147.

776 Van Genuchten, M.Th, 1981. Analytical solutions for chemical transport with simultaneous
777 adsorption, zero-order production and first order decay. *J. Hydrol.* 49, 213–233.
778 [https://doi.org/10.1016/0022-1694\(81\)90214-6](https://doi.org/10.1016/0022-1694(81)90214-6)

779 Wang, H.Q., Crampon, N., 1995. Method for interpreting tracer experiments in radial flow
780 using modified analytical solutions. *J. Hydrol.* 165(1-4), 11–31.
781 [https://doi.org/10.1016/0022-1694\(94\)02588-3](https://doi.org/10.1016/0022-1694(94)02588-3)

782 Wang, Q., Zhan, H., 2013. Radial reactive solute transport in an aquifer–aquitard system.
783 *Advances in Water Resources*, 61(2013): 51-61.
784 <http://dx.doi.org/10.1016/j.advwatres.2013.08.013>

785 Welty, C., Gelhar, L.W., 1994. Evaluation of longitudinal dispersivity from nonuniform flow
786 tracer tests. *J. Hydrol.* 153, 71–102. [https://doi.org/10.1016/0022-1694\(94\)90187-2](https://doi.org/10.1016/0022-1694(94)90187-2)

787 Zlotnik, V.A., Logan, J.D., 1996. Boundary conditions for convergent radial tracer tests and
788 the effect of well bore mixing volume. *Water Resour. Res.* 32 (7), 2323–2328.

Figure and table captions for manuscript HYDROL43236:

D. Thiéry (2022) - Simple approximate closed-form expressions for tracer injection in aquifer with a radially converging or diverging flow field.

Figure captions

Fig. 1. Schematic diagram of radially diverging (left) or converging (right) tracer test. (Q is pumped or injected flow rate, q_m is injected or mass flux, M is injected mass, h is aquifer thickness, ω is kinematic porosity, r_L is radial distance from center well to outer well, $C(t)$ is concentration as a function of time).

Fig. 2. Comparison of dimensional BTCs obtained with the numerical model to the Chen et al. (1996) solution, in a hypothetical condition in converging flow in unbounded domain.

Fig. 3. 2D numerical simulation with transverse dispersivity in converging flow: comparison with a 1D radial simulation. (Péclet number = 5, transverse dispersivity = $0.2 \times \alpha_L$).

Fig. 4. Comparison of the numerical solution for a slug injection in unbounded domain in converging flow and in diverging flow in dimensionless coordinates.

Fig. 5. Comparison of the numerical simulation of a slug injection in unbounded domain in converging flow and in diverging flow for a Péclet number equal to 3; $t_D=0.25$ & $t_D=0.5$. Left: diverging flow; right converging flow.

Fig. 6. Comparison of the numerical solution for a slug injection in bounded domain in converging and in diverging flow in dimensionless coordinates.

Fig. 7. Comparison of the numerical simulation of a slug injection in bounded domain in converging flow and in diverging flow for a Péclet number equal to 3; $t_D=0.25$ & $t_D=0.4$. Left: diverging flow; right converging flow.

Fig. 8. Continuous injection in unbounded domain, converging flow and diverging flow.

Fig. 9. Slug injection in unbounded domain in converging flow or diverging flow.

Fig. 10. Continuous injection in bounded domain, converging flow and diverging flow.

Fig. 11. Slug injection in bounded domain in converging flow or diverging flow.

Fig. 12. Slug injection in converging flow or diverging flow in unbounded domain with various dimensionless decay time constants T_{gD} . Left: Péclet number = 2; Right: Péclet number = 10.

Fig. 13. Twelve field tracer tests: deviations in kinematic porosity (upper part) and dispersivity (lower part) using the formulation of Wang & Crampon (1995) compared to using the new quasi exact closed form approximation in unbounded domain.

Fig. A1. Dimensionless BTCs in a bounded domain in a converging flow obtained with the numerical model [solid line], compared with the solution of Chen et al. (2002) [symbols]. Péclet numbers from 0.1 to 25.

Fig. A2. Dimensionless BTCs in a bounded domain in a converging flow obtained with the numerical model [solid line], compared with the solution of Chen et al. (2002) [symbols]. Péclet numbers from 25 to 200.

Fig. B1. Exact solution of BTCs in radial bounded domain compared to: A) Sauty's (1980) approximate solution; B) This paper new closed-form approximation.

Fig. B2. Exact solution of BTCs in radial unbounded domain compared to: A) the approximate solution of Wang and Crampon (1995); B) this paper new closed-form approximation.

Fig. C1. Exact solution in bounded domain: calibration in unbounded domain with modified parameters.

Fig. C2. Exact solution in bounded domain: modification of the porosity and dispersivity resulting from a calibration in unbounded domain.

Table captions

Table 1. Characteristics of the 12 radially convergent tracer tests.

Table 2. Transfer parameters obtained for the 12 tracer tests using the new closed-form expression in unbounded domain.

Table 3. Transfer parameters obtained for the 12 tracer tests using the expression of Wang & Crampon (1995), and deviations from the new closed-form expression in unbounded domain.

D. Thiéry (2022) - Simple approximate closed-form expressions for tracer injection in aquifer with a radially converging or diverging flow field.

Note: Most of the figures can be reduced to a smaller size in the edited paper.

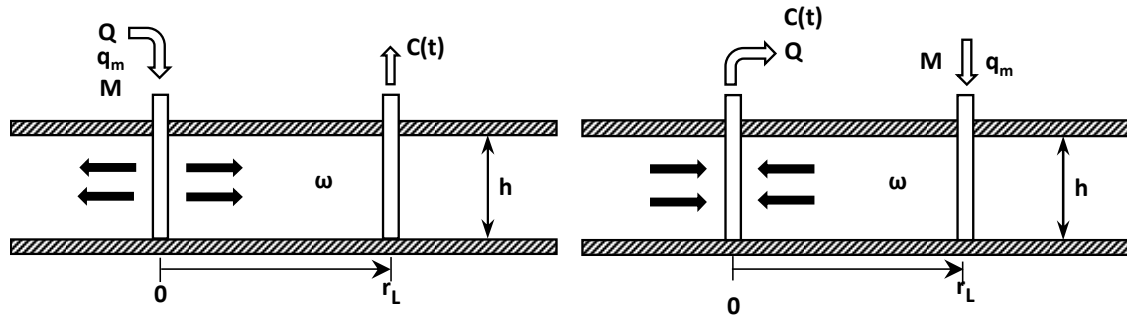


Fig. 1. Schematic diagram of radially diverging (left) or converging (right) tracer test. (Q is pumped or injected flow rate, q_m is injected or mass flux, M is injected mass, h is aquifer thickness, ω is kinematic porosity, r_L is radial distance from center well to outer well, $C(t)$ is concentration as a function of time).

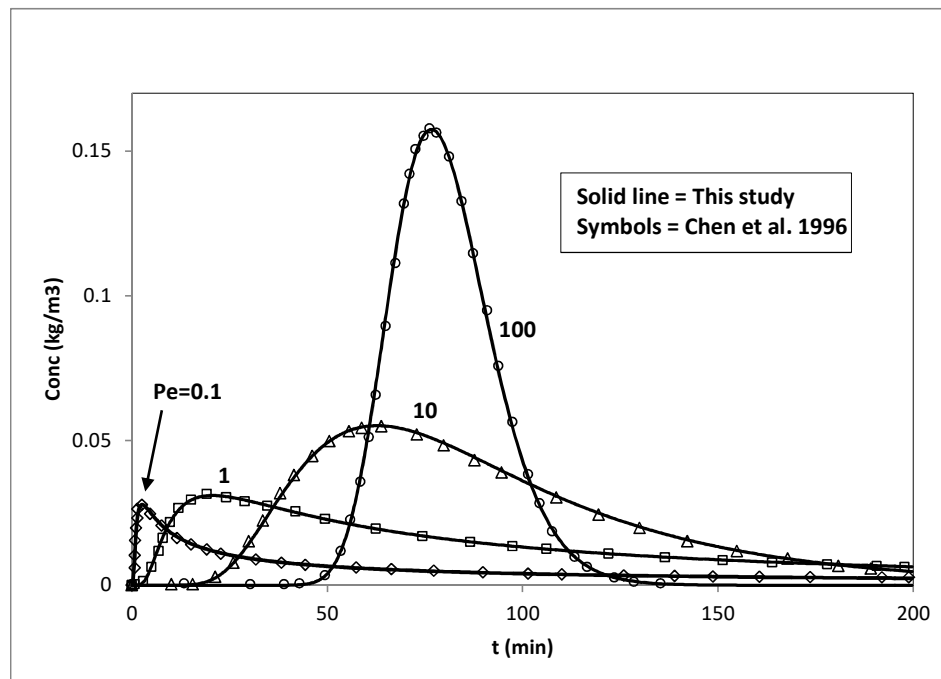


Fig. 2. Comparison of dimensional BTCs obtained with the numerical model to the Chen et al. (1996) solution in a hypothetical condition in converging flow in unbounded domain.

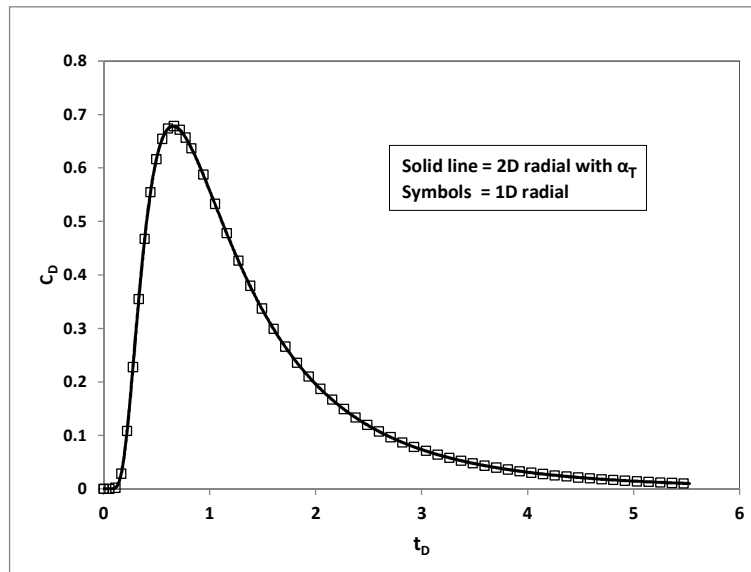


Fig. 3. 2D numerical simulation with transverse dispersivity in converging flow: comparison with a 1D radial simulation. (Péclet number = 5, transverse dispersivity = $0.2 \times \alpha_L$).

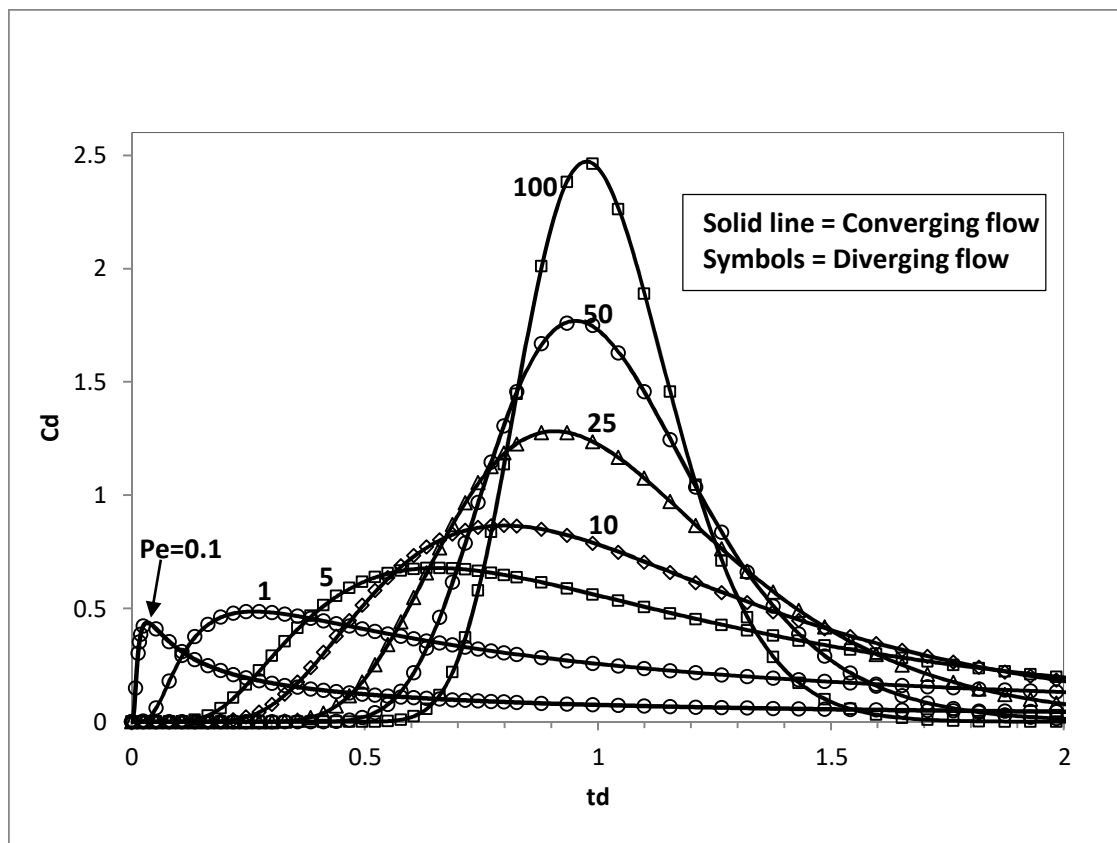


Fig. 4. Comparison of the numerical solution for a slug injection in unbounded domain in converging flow and in diverging flow in dimensionless coordinates.

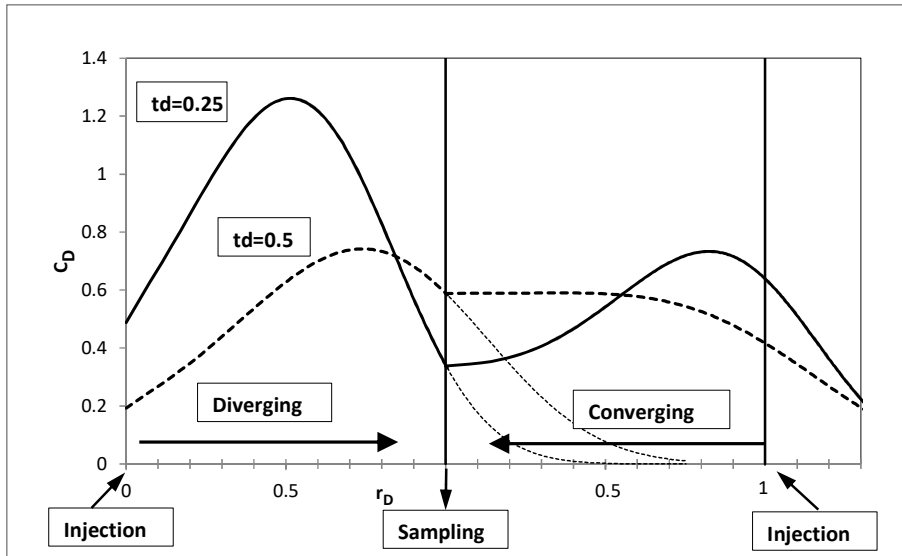


Fig. 5. Comparison of the numerical simulation of a slug injection in unbounded domain in converging flow and in diverging flow for a Péclet number equal to 3; $t_D=0.25$ & $t_D=0.5$. Left: diverging flow; right converging flow.

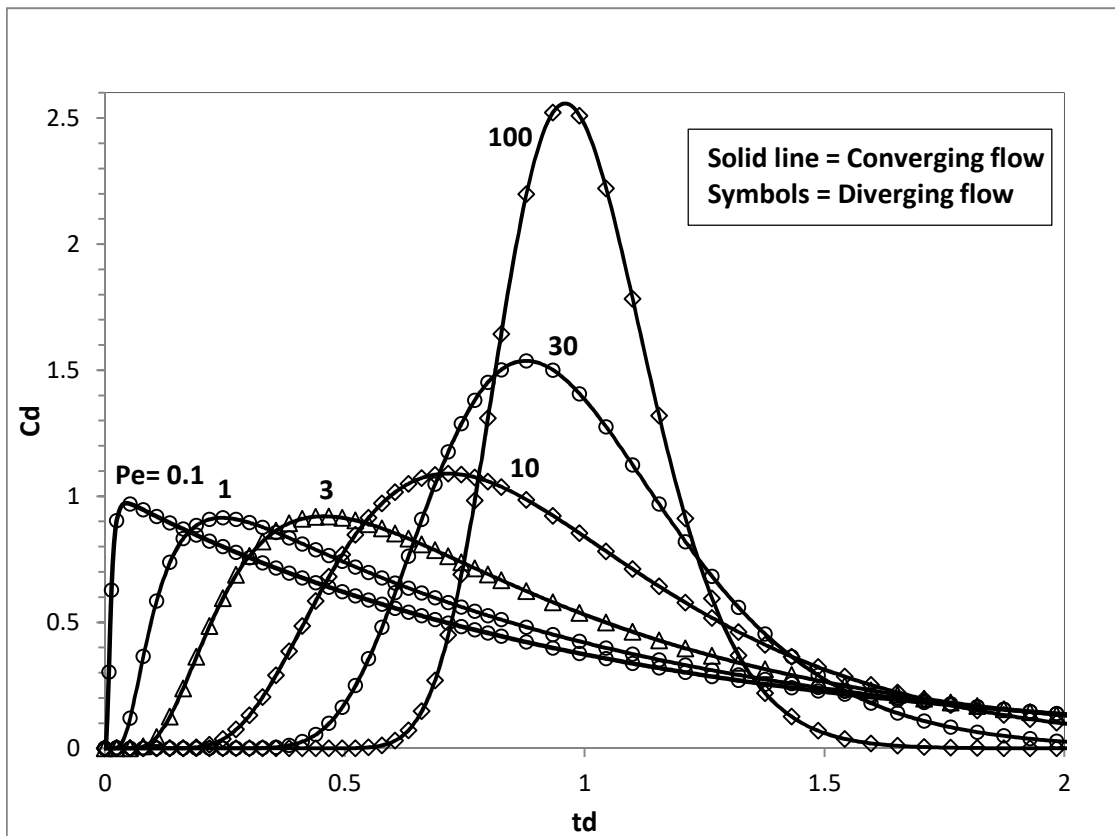


Fig. 6. Comparison of the numerical solution for a slug injection in bounded domain in converging and in diverging flow in dimensionless coordinates.

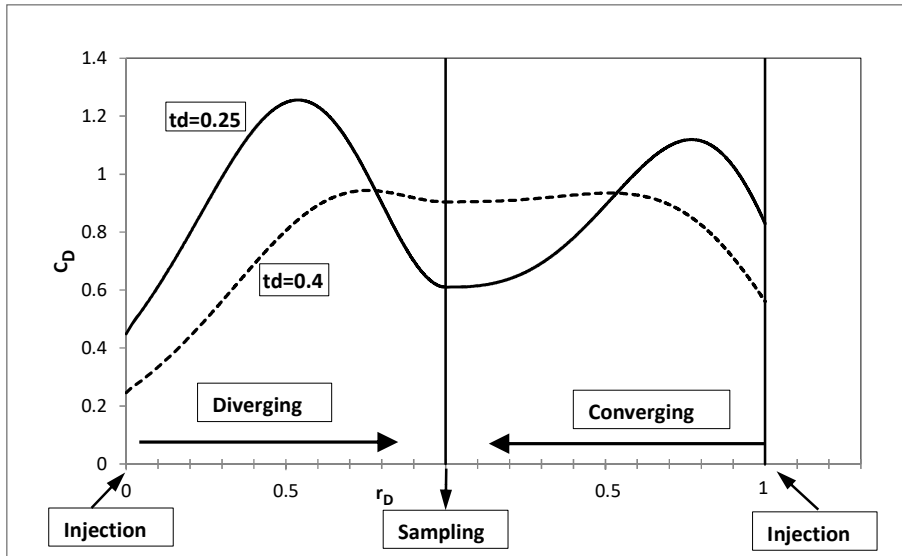


Fig. 7. Comparison of the numerical simulation of a slug injection in bounded domain in converging flow and in diverging flow for a Péclet number equal to 3; $t_D=0.25$ & $t_D=0.4$. Left: diverging flow; right converging flow.

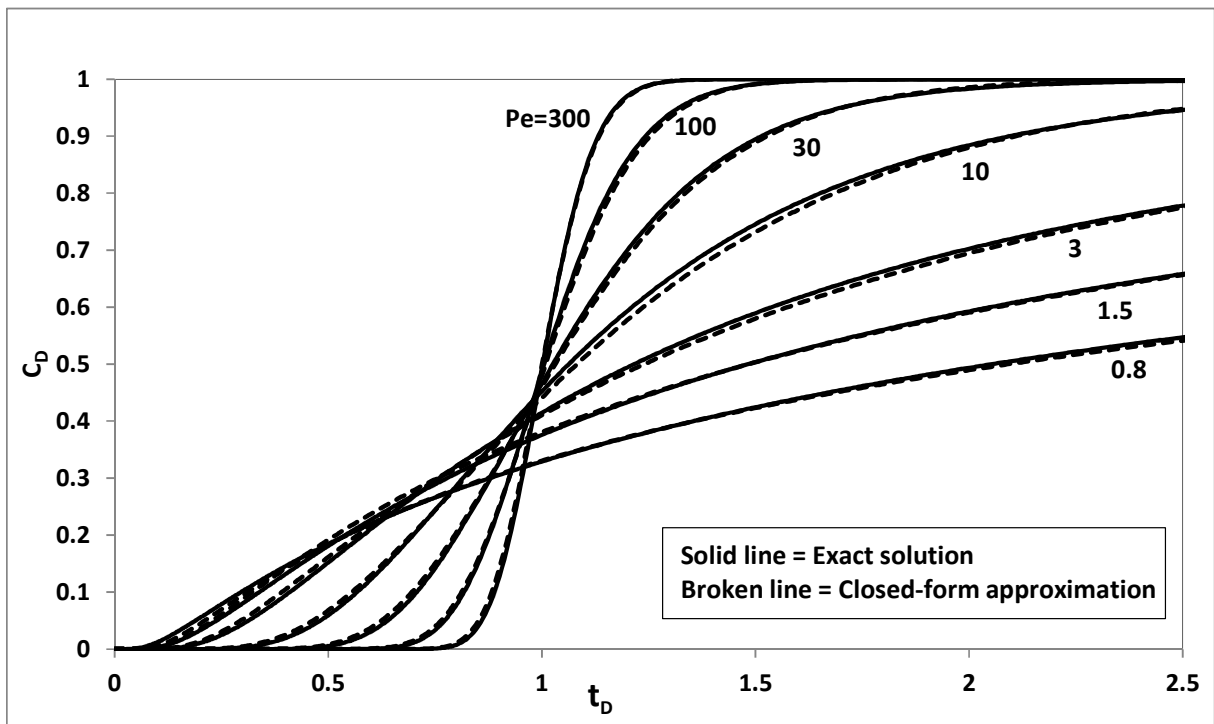


Fig. 8. Continuous injection in unbounded domain, converging flow and diverging flow.

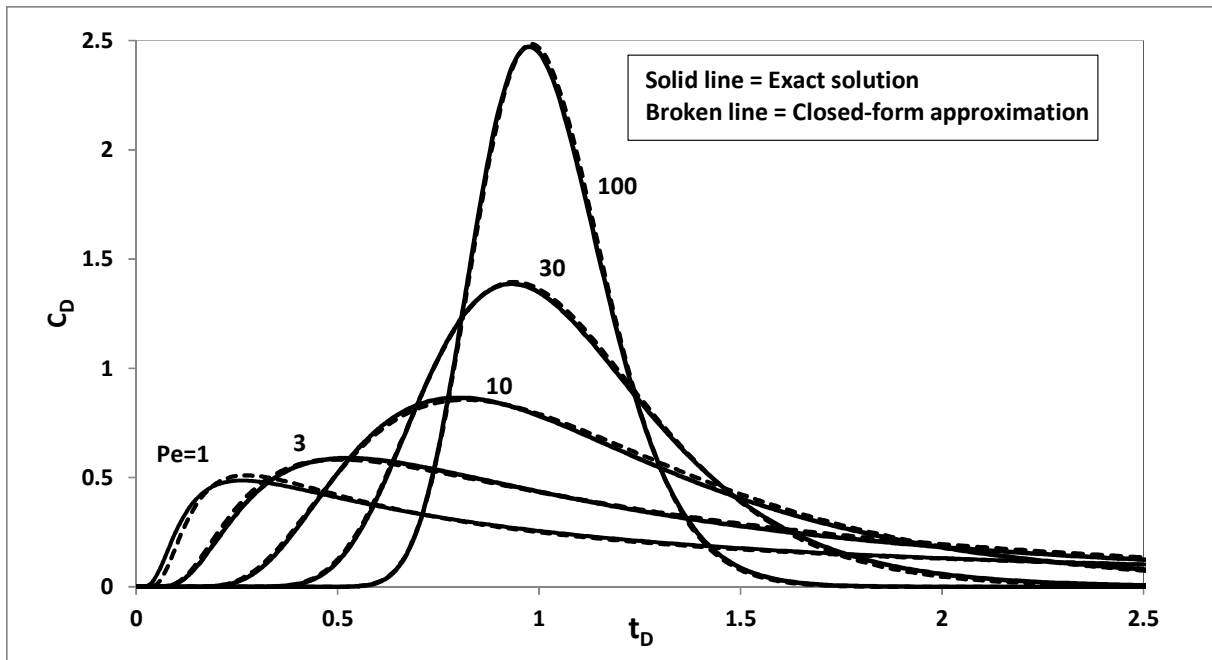


Fig. 9. Slug injection in unbounded domain in converging flow or diverging flow.

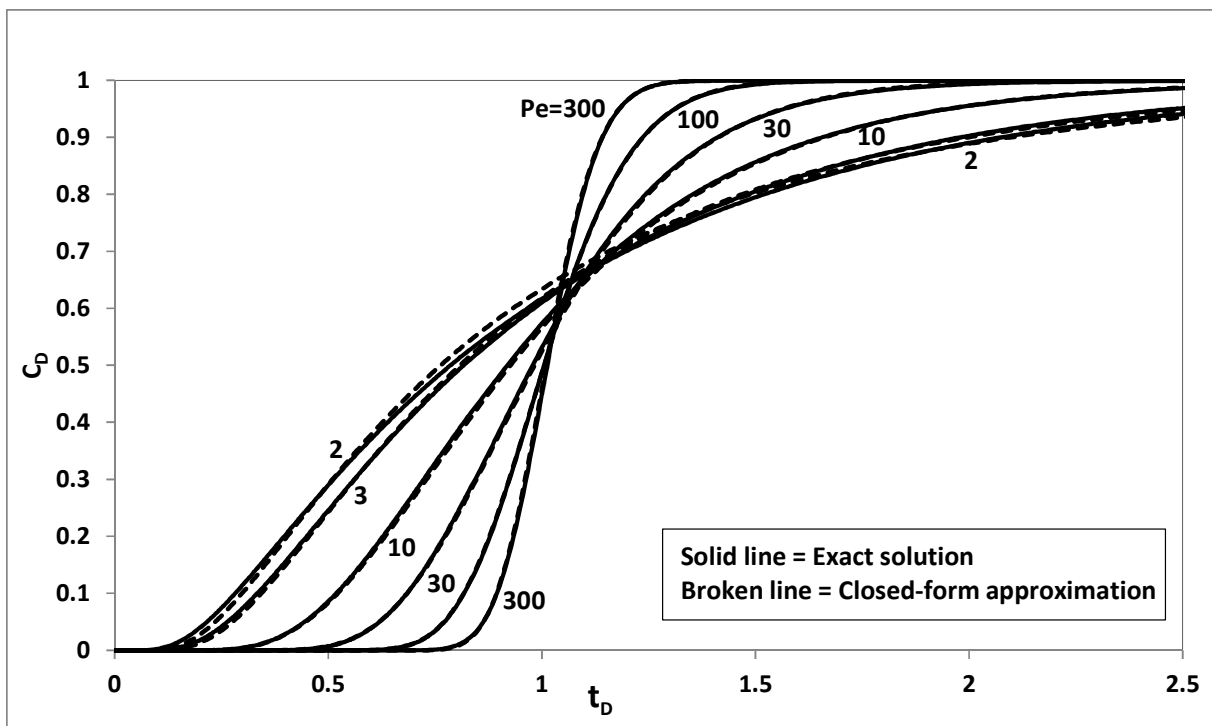


Fig. 10. Continuous injection in bounded domain, converging flow and diverging flow.

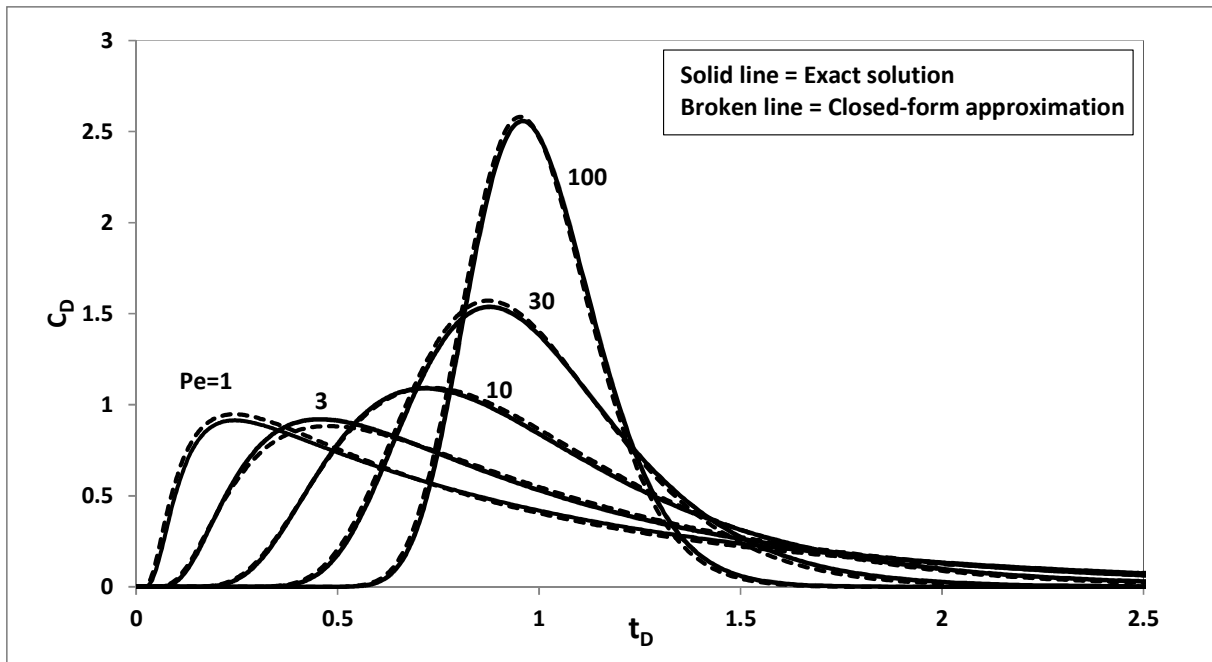


Fig. 11. Slug injection in bounded domain in converging flow or diverging flow.

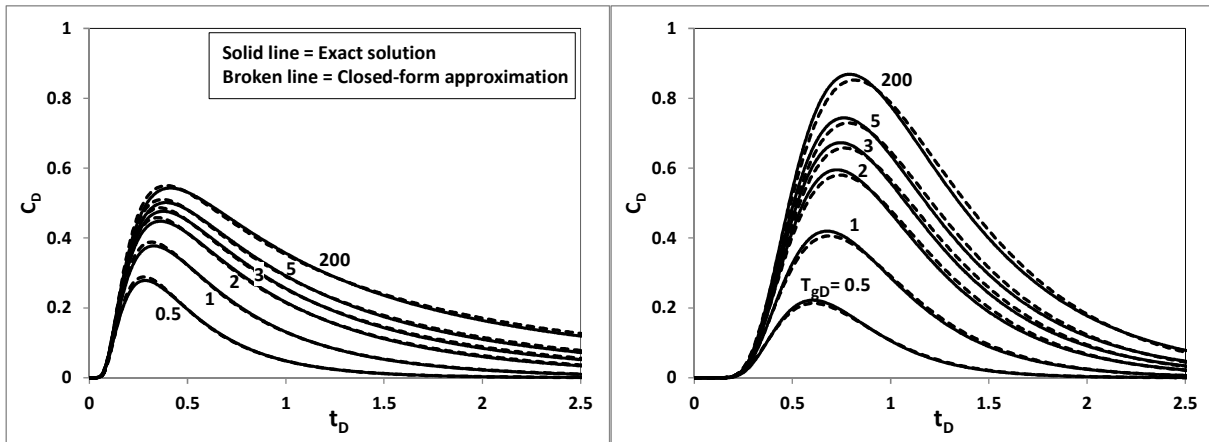


Fig. 12. Slug injection in converging flow or diverging flow in unbounded domain with various dimensionless decay time constants T_{gD} . Left: Péclet number = 2; Right: Péclet number = 10.

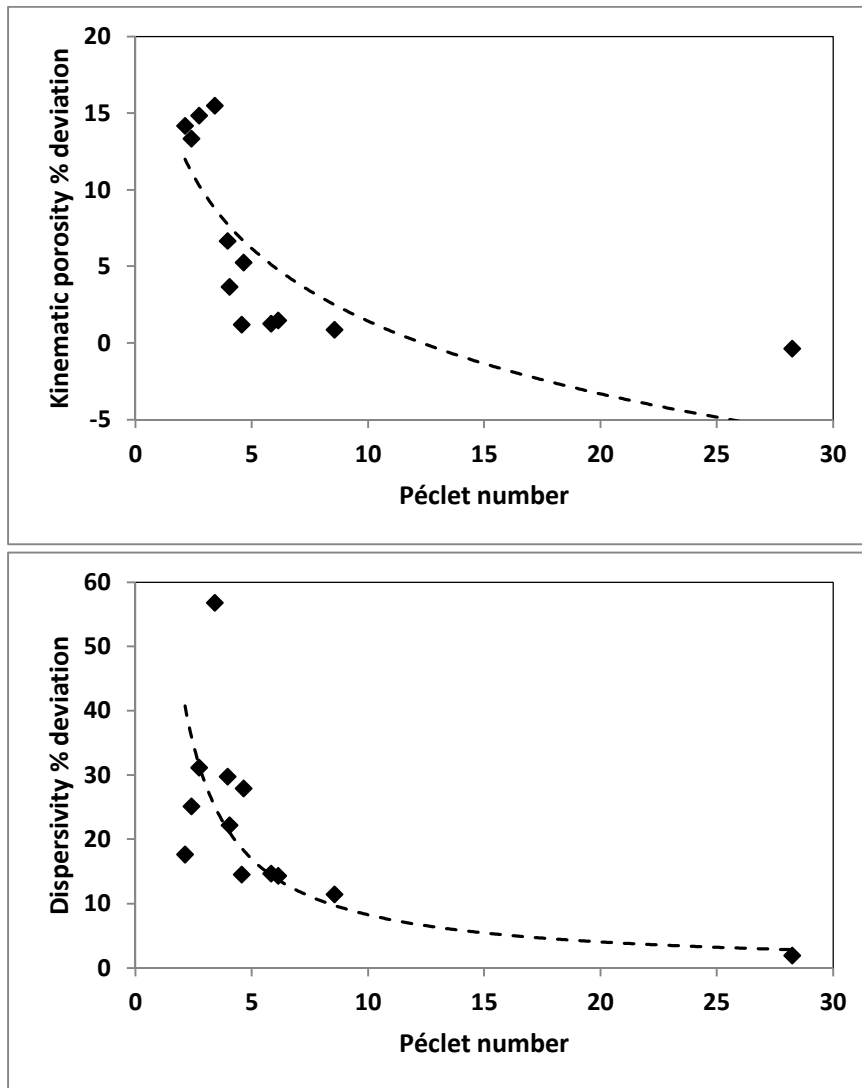


Fig. 13. Twelve field tracer tests: deviations in kinematic porosity (upper part) and dispersivity (lower part) using the formulation of Wang & Crampon (1995) compared to using the new quasi exact closed form approximation in unbounded domain.

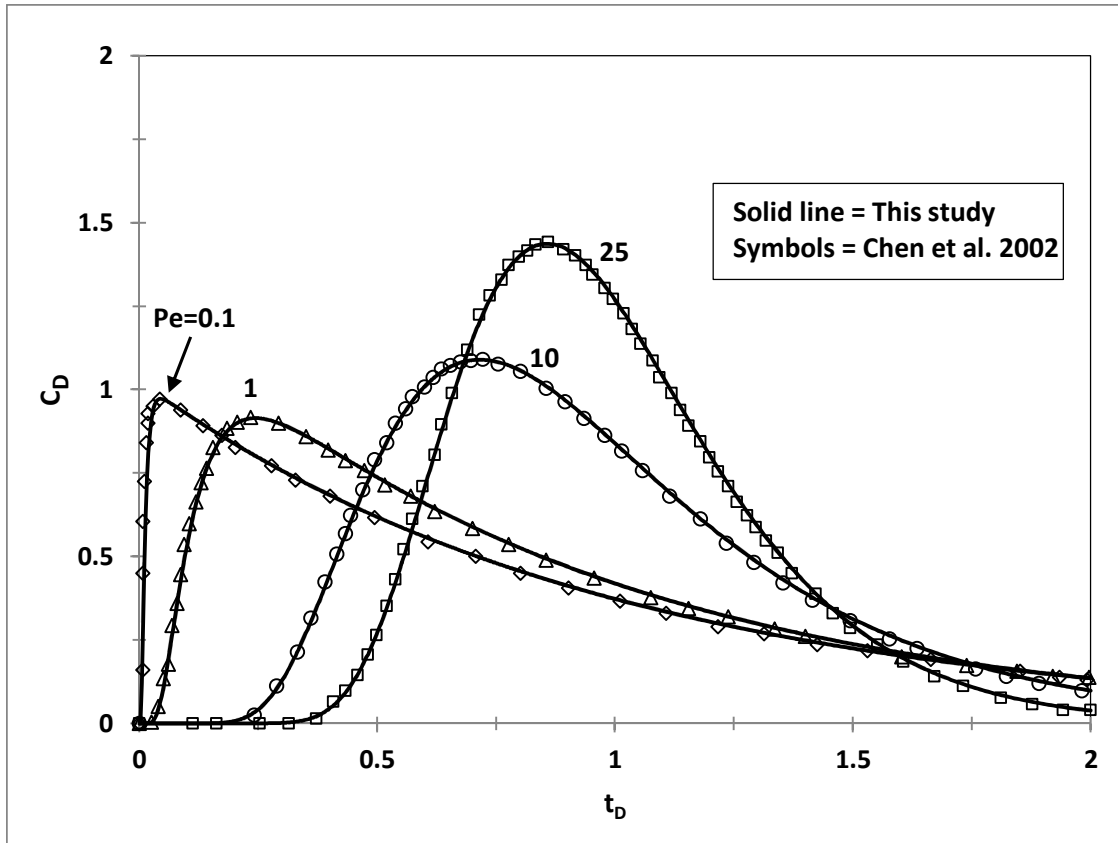


Fig. A1. Dimensionless BTCs in a bounded domain in a converging flow obtained with the numerical model [solid line], compared with the solution of Chen et al. (2002) [symbols]. Péclet numbers from 0.1 to 25.

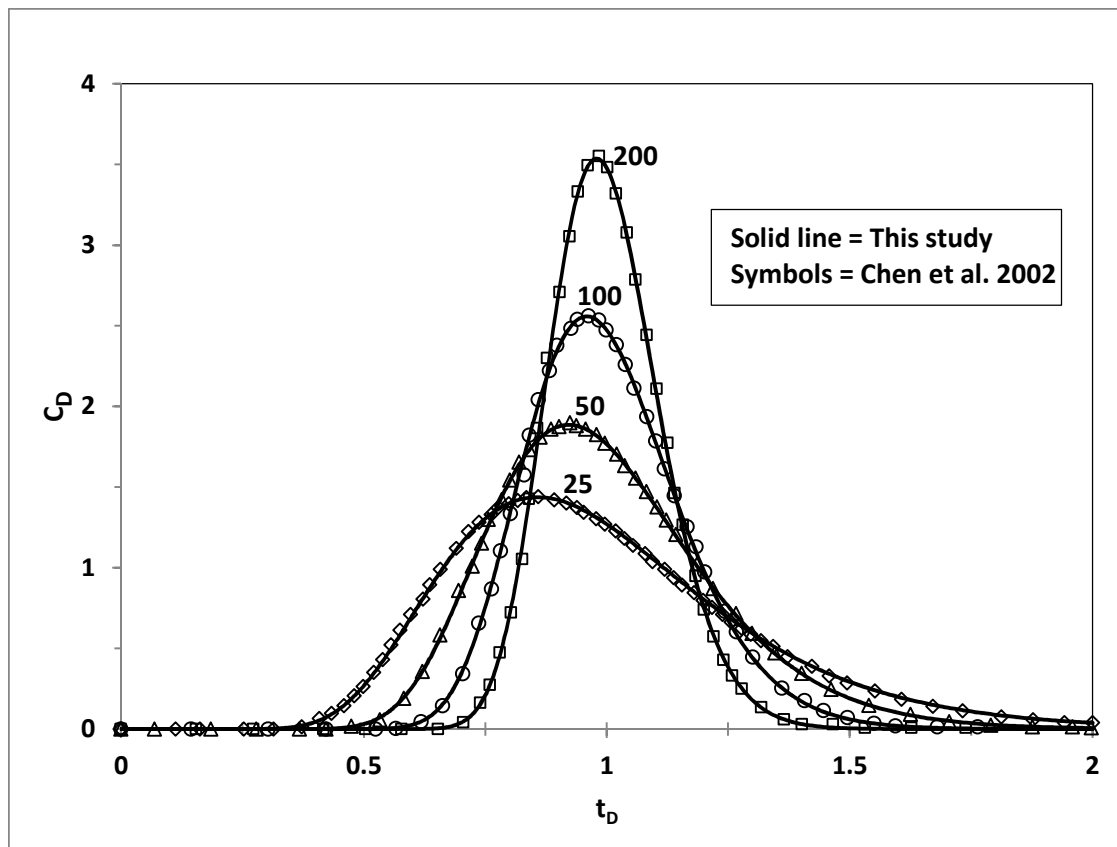


Fig. A2. Dimensionless BTCs in a bounded domain in a converging flow obtained with the numerical model [solid line], compared with the solution of Chen et al. (2002) [symbols]. Péclet numbers from 25 to 200.

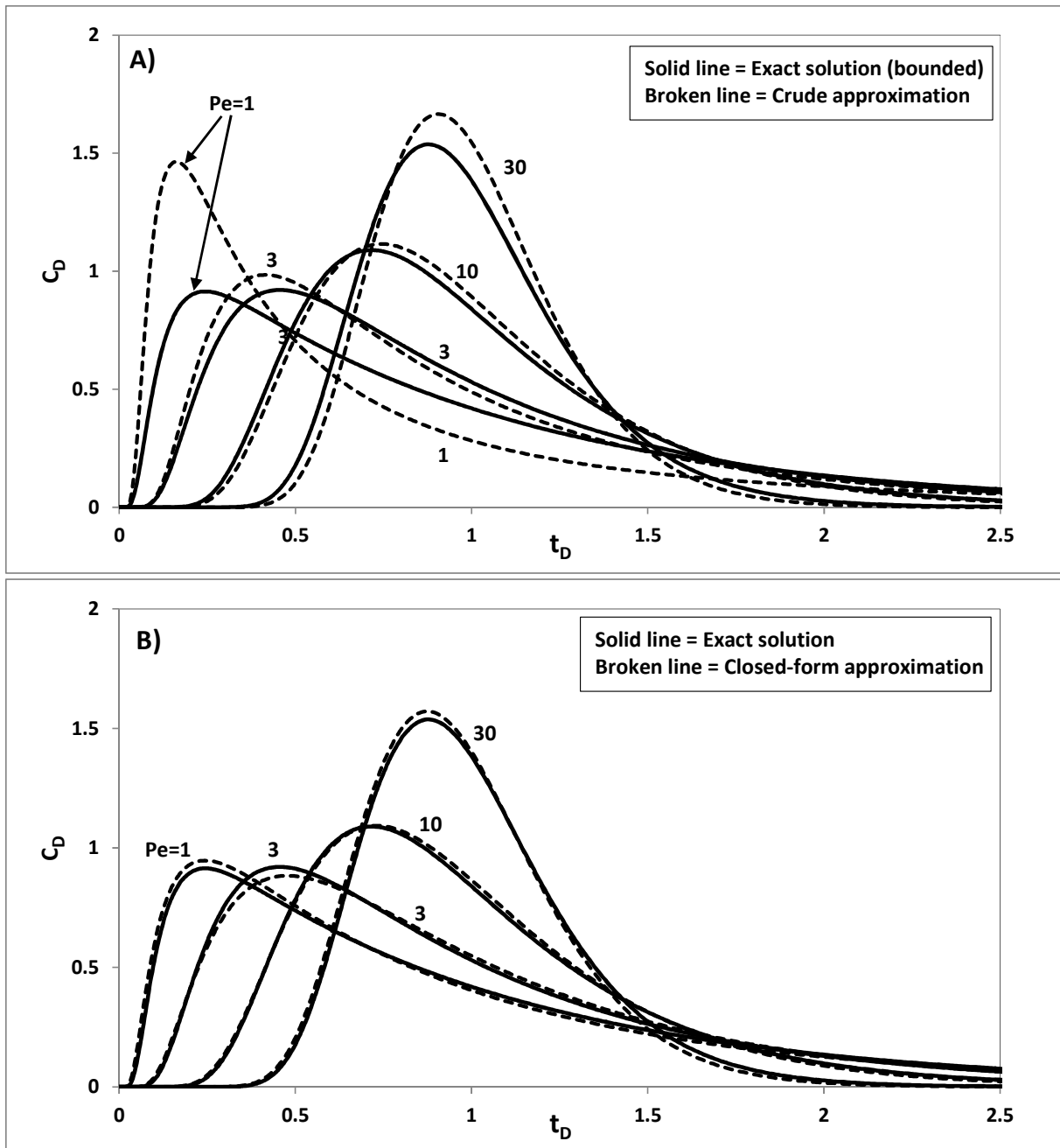


Fig. B1. Exact solution of BTCs in radial bounded domain compared to: A) Sauty's (1980) approximate solution; B) this paper new closed-form approximation.

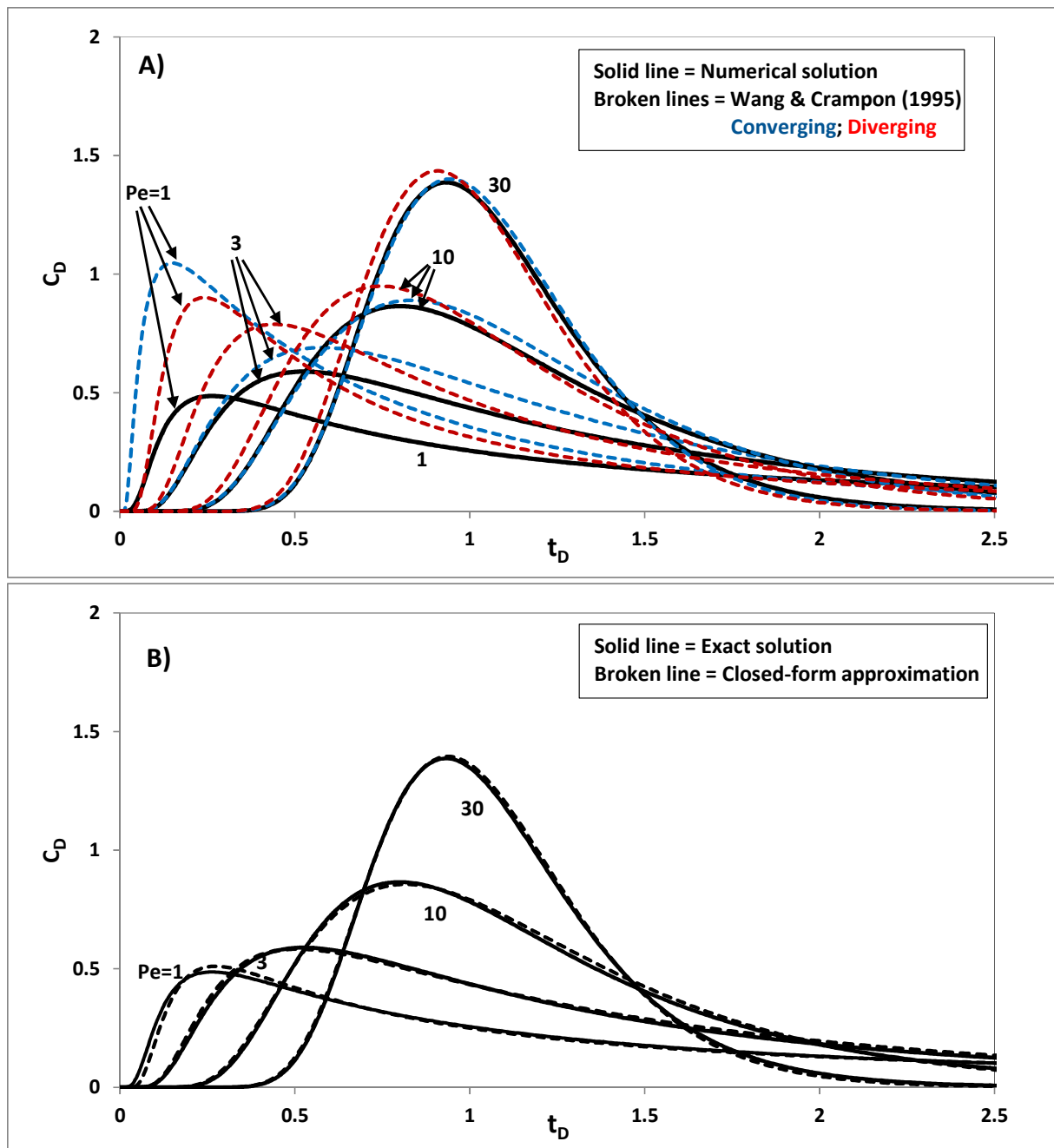


Fig. B2. Exact solution of BTCs in radial unbounded domain compared to: A) the approximate solution of Wang and Crampon (1995); B) this paper new closed-form approximation.

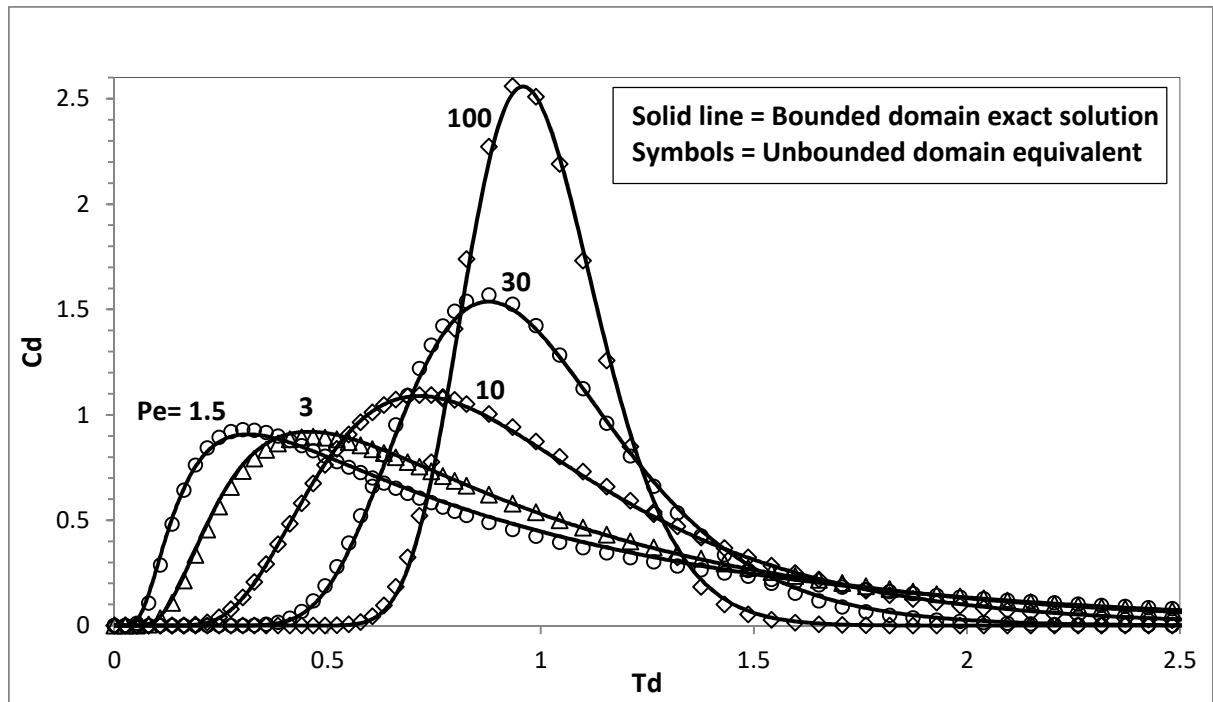


Fig. C1. Exact solution in bounded domain: calibration in unbounded domain with modified parameters.

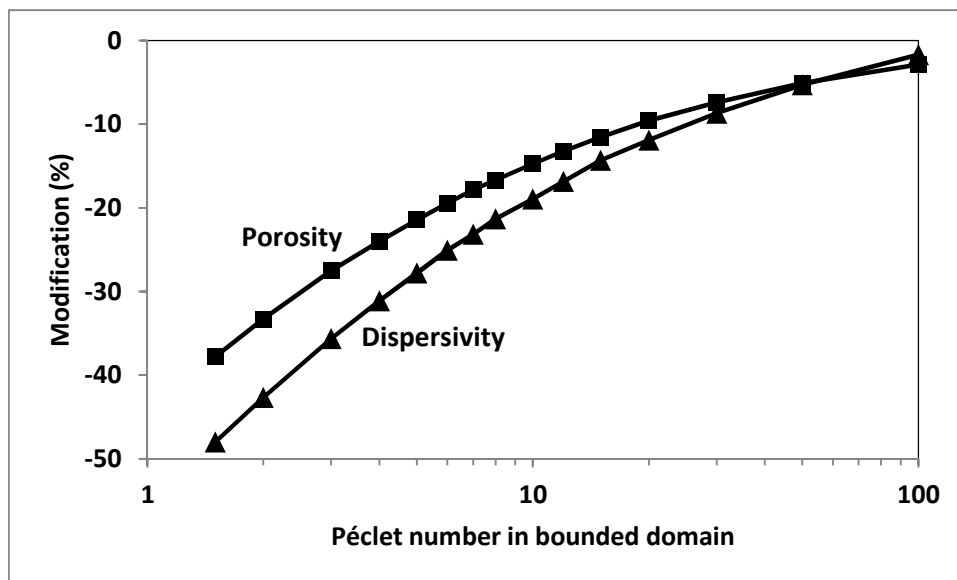


Fig. C2. Exact solution in bounded domain: modification of the dispersivity and porosity resulting from a calibration in unbounded domain.

Nomenclature

Notation	Definition	Unit	Relation
A	Intermediate variable	L^2T^{-1}	$A = Q / 2\pi h\omega$
C	Concentration	ML^{-3}	
C_D	Dimensionless concentration	-	$C_D = C/C_{ref}$ or C/C_0
C_{ref}	Reference concentration	ML^{-3}	$C_{ref} = M/(\pi r_L^2 h\omega)$
C_0	Injected concentration	ML^{-3}	$C_0 = q_m/Q$
D_L	Longitudinal dispersion coefficient	L^2T^{-1}	$D_L = \alpha_L u $
erfc()	Complementary error function	-	
F	Slug injection: F=0; continuous injection: F=1	-	
f_P	Correcting factors for Péclet number	-	
f_T	Correcting factors for dimensionless time	-	
h	Aquifer thickness	L	
K	Normalization constant	-	
M	Injected mass	M	
P	Péclet number	-	$P = r_L / \alpha_L$
Q	Injected or pumped flow rate	L^3T^{-1}	
q_m	Mass flux	MT^{-1}	
R	Retardation coefficient	-	
r	Radial distance	L	
r_D	Dimensionless radial distance	-	$r_D = r / r_L$
r_L	Radial distance to outer well	L	
t	Time	T	
t_a	Advection time from outer to center	T	$t_a = \pi r_L^2 h\omega / Q$
t_D	Dimensionless time	-	$t_D = t / t_a$
T_g	First-order decay time constant	T	$T_g = 1/\lambda$
T_{gD}	Dimensionless decay time constant	-	$T_{gD} = T_g / t_a$
u	Pore velocity	LT^{-1}	
α_L	Longitudinal dispersivity	L	
α_T	Transverse dispersivity	L	
ε	Diverging flow: +1; converging flow: -1	-	
θ	Angular coordinate	-	
λ	First-order decay constant	T^{-1}	
ω	Kinematic porosity	-	

Table 1
 Characteristics of the 12 radially convergent tracer tests

No	Distance to well	Formation thickness	Pumping rate	Duration of test	Name
	m	m	m ³ /h	hour	
1	13.9	6.25	39.5	49	Ginger_1
2	15	10	38.5	46	Ginger_2
3	12	8.5	22	24	Ginger_3
4	20	8.5	22	22	Ginger_4
5	20	10.35	24.1	30	Astaillac
6	19.5	10.35	24.1	28.4	Astaillac
7	14.43	8	45	47.3	Tauriac
8	14.04	11	25	48	Bretenoux
9	7.9	11	25	47.9	Bretenoux
10	13	2.5	3.5	177.7	Bonaud Ina (09/1977)
11	9	2	4	45.6	Test_4 (Sauty 1977)
12	200	12	138.6	502	South Farm (Atkinson 2000)
Median	14	9.3	24.6	46.7	

Table 2

Transfer parameters obtained for the 12 tracer tests using the new closed-form expression in unbounded domain.

No	Dispersivity α_L	Kinematic porosity	Péclet number r_L / α_L	Injected mass	Nash coefficient
unit	m	[-]	[-]	g	[-]
1	0.49	0.186	28.2	0.6	0.996
2	6.21	0.036	2.42	191	0.996
3	3.03	0.014	3.96	173	0.945
4	4.30	0.017	4.65	50.4	0.987
5	9.38	0.020	2.13	36.9	0.979
6	7.12	0.012	2.74	38.9	0.972
7	2.47	0.141	5.84	217	0.895
8	3.47	0.063	4.04	222	0.974
9	1.73	0.068	4.57	0.698	0.974
10	1.52	0.078	8.56	137	0.994
11	2.64	0.106	3.41	34.8	0.999
12	32.6	0.014	6.14	144	0.932
Median	3.3	0.049	4.3	93.7	0.977

Table 3

Transfer parameters obtained for the 12 tracer tests using the expression of Wang & Crampon (1995), and deviations from the new closed-form expression in unbounded domain.

No	Dispersivity α_L m	Dispersivity α_L % deviation	Kinematic porosity [-]	Kinematic porosity % deviation	Péclet number (reference) [-]
1	0.50	1.9	0.185	-0.4	28.2
2	7.77	25	0.041	13	2.4
3	3.93	30	0.015	6.7	4.0
4	5.50	28	0.017	5.2	4.7
5	11.0	18	0.023	14	2.1
6	9.33	31	0.013	15	2.7
7	2.83	15	0.142	1.3	5.8
8	4.24	22	0.065	3.7	4.0
9	1.98	15	0.069	1.2	4.6
10	1.69	12	0.079	0.9	8.6
11	4.13	57	0.123	15	3.4
12	37.3	14	0.014	1.5	6.1
Median	4.2	19.9	0.053	4.4	4.3